Copyright Warning & Restrictions

The copyright law of the United States (Title 17, United States Code) governs the making of photocopies or other reproductions of copyrighted material.

Under certain conditions specified in the law, libraries and archives are authorized to furnish a photocopy or other reproduction. One of these specified conditions is that the photocopy or reproduction is not to be "used for any purpose other than private study, scholarship, or research." If a, user makes a request for, or later uses, a photocopy or reproduction for purposes in excess of "fair use" that user may be liable for copyright infringement,

This institution reserves the right to refuse to accept a copying order if, in its judgment, fulfillment of the order would involve violation of copyright law.

Please Note: The author retains the copyright while the New Jersey Institute of Technology reserves the right to distribute this thesis or dissertation

Printing note: If you do not wish to print this page, then select "Pages from: first page # to: last page #" on the print dialog screen

ABSTRACT

COMPARISON OF LONGITUDINAL CHANGES IN RESTING STATE FUNCTIONAL MAGNETIC RESONANCE IMAGING BETWEEN ALZHEIMER'S PATIENTS AND HEALTHY CONTROLS

by
Berk Can Yilmaz

Resting State Functional Magnetic Resonance Imaging (rs-fMRI) is a technique that is widely used for analyzing brain function using different approaches and methods. This study involves rs-fMRI analysis of Blood Oxygenation Level Dependent (BOLD) signals acquired from Alzheimer's disease (AD) Patients and Healthy Controls (HC). Each subject in the study had both functional and anatomical images with at least one rs-fMRI scan with their Anatomical (T1) scans. Previous rs-fMRI studies have demonstrated that AD shows differences in Amplitude of Low Frequency (<0.1 Hz) Fluctuations (ALFF), and Regional Homogeneity (ReHo) measures according to HCs.

The aim of the study is to investigate individual and group level differences using ReHo and mALFF related measures in a longitudinal analysis. The hypothesis is that with the age and group (AD or HC) of the subject, it is possible to separate AD and HC subjects from each other using 3 different ROIs (DMN – MT – MV), These regions are known to show abnormalities in AD patients but clinical wise never been identified as neuroimaging biomarkers. This study tries to check these ROIs to see if there are significant differences between the AD patients and HCs using 3 different features.

COMPARISON OF LONGITUDINAL CHANGES IN RESTING STATE FUNCTIONAL MAGNETIC RESONANCE IMAGING BETWEEN ALZHEIMER'S AND HEALTHY CONTROLS

by
Berk Can Yilmaz

A Thesis
Submitted to the Faculty of
New Jersey Institute of Technology
in Partial Fulfillment of the Requirements for the Degree of
Master of Science in Biomedical Engineering

Department of Biomedical Engineering

August 2020

APPROVAL PAGE

COMPARISON OF LONGITUDINAL CHANGES IN RESTING STATE FUNCTIONAL MAGNETIC RESONANCE IMAGING BETWEEN ALZHEIMER'S AND HEALTHY CONTROLS

Berk Can Yilmaz

Dr. Bharat B. Biswal, Thesis Advisor — Date
Distinguished Professor Biomedical Engineering, NJIT

Dr. Sergei Adamovich, Committee Member — Date
Professor of Biomedical Engineering, NJIT

Dr. Xiabo Li, Committee Member — Date
Associate Professor of Biomedical Engineering, NJIT

Dr. Xin Di, Committee Member — Date
Research Professor of Biomedical Engineering, NJIT

BIOGRAPHICAL SKETCH

Author: Berk Can Yilmaz

Degree: Master of Science

Date: August 2020

Undergraduate and Graduate Education:

- Master of Science in Biomedical Engineering,
  New Jersey Institute of Technology, Newark, New Jersey, 2020

- Bachelor of Science in Biomedical Engineering,
  Baskent University, Ankara, 2016

Major: Biomedical Engineering

To my parents… the reason of my existence and who I am for better or worse.

To my brothers from football… crucial part of my life where I learned the importance and value of hard work.

To my sister Ceren Gul Yilmaz… still hoping we will get close again one day as brother and sister.

To my uncle and my aunt… my second father and my second mother.

To Donna and Shruti… Thank you for all your support.

To Irina… My new sister, thank you coming into my life.

"If one day, my words are against science, choose science."

— Mustafa Kemal Atatürk

"Nothing is an absolute reality; all is permitted"

– Vladimir Bartol

"VI VERI VENIVERSUM VIVUS VICI"

– Alan Moore

"However, they asked many times: What will happen when you grow up? We couldn't say "Happy". Because we were children; we couldn't think of…."

– Nazım Hikmet

ACKNOWLEDGMENT

I would like to express my gratitude to my advisor Dr. Bharat B. Biswal and Dr. Xin Di for their teachings, patience and support. I would also like to thank Dr. Max Roman and my committee members including Dr. Xiaobo Li and Dr. Sergei Adamovich for their teachings, patience and their insights on my project.

I am also very grateful for every lab member of mine at NJIT Brain Connectivity Lab. I would like to thank Hafiz for everything he taught me and being my big brother, Donna for your support and being a younger sister, Azeezat and Keerthana for their time and everything they taught me, Katherine, Shruti, Avininjra, Tom, and Jonas for being so kind and supporting. I am really glad, honored, and lucky to get to know each and every one of you.

TABLE OF CONTENTS

TABLE OF CONTENTS
(Continued)

LIST OF FIGURES

LIST OF FIGURES
(Continued)

Figure **Page**

LIST OF TABLES

Table **Page**

CHAPTER 1

INTRODUCTION

1.1 Alzheimer's Disease

This current study focuses on functional brain activity in Alzheimer's disease (AD) patients and compares against healthy control subjects. AD, discovered and named after German psychiatrist Dr. Alois Alzheimer, is a progressive neurodegenerative disease that affects older people (>50 years old). His patient, Auguste D., experienced memory loss, paranoia, psychological changes, and cognitive impairment. During the autopsy, Dr. Alzheimer found abnormalities in the white matter (WM) of the AD patient's brain (Azeez & Biswal, 2017, Hippius & Neundörfer, 2003, Giffard et al., 2008). Figure 1 presents a representation of the known risk factors associated with AD.

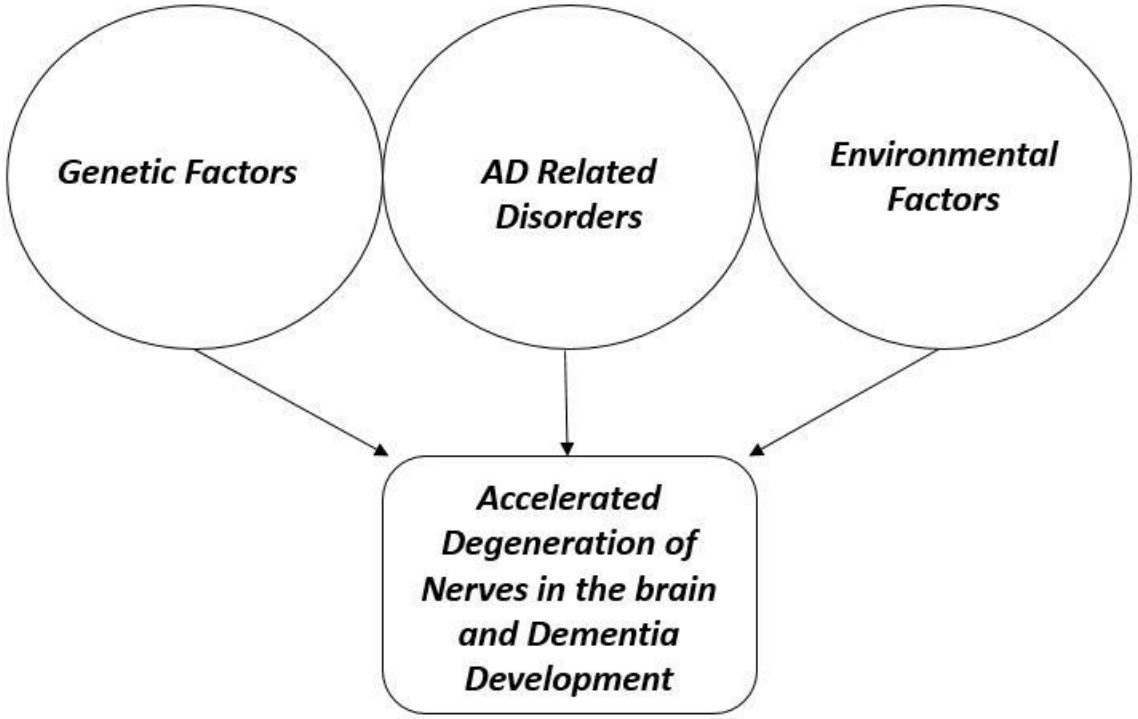

Figure 1.1 Alzheimer's disease risk factors.

AD patients experience psychiatric symptoms and dementia that gradually progress with age (Onyike, 2017), as represented in Figure 1.2. A recent study by Xia-a Bi and colleagues showed that the number of AD patients worldwide could potentially reach one hundred million by 2050 (Bi et al., 2018). This necessitates the importance of having an early detection mechanism. Biomarkers in neuroimaging provide the opportunity to improve early detection by identifying changes that occur with the progression of psychiatric symptoms and dementia (Onyike, 2017). For AD specifically, early detection can be improved by identifying changes in cognitive function with neuroimaging.

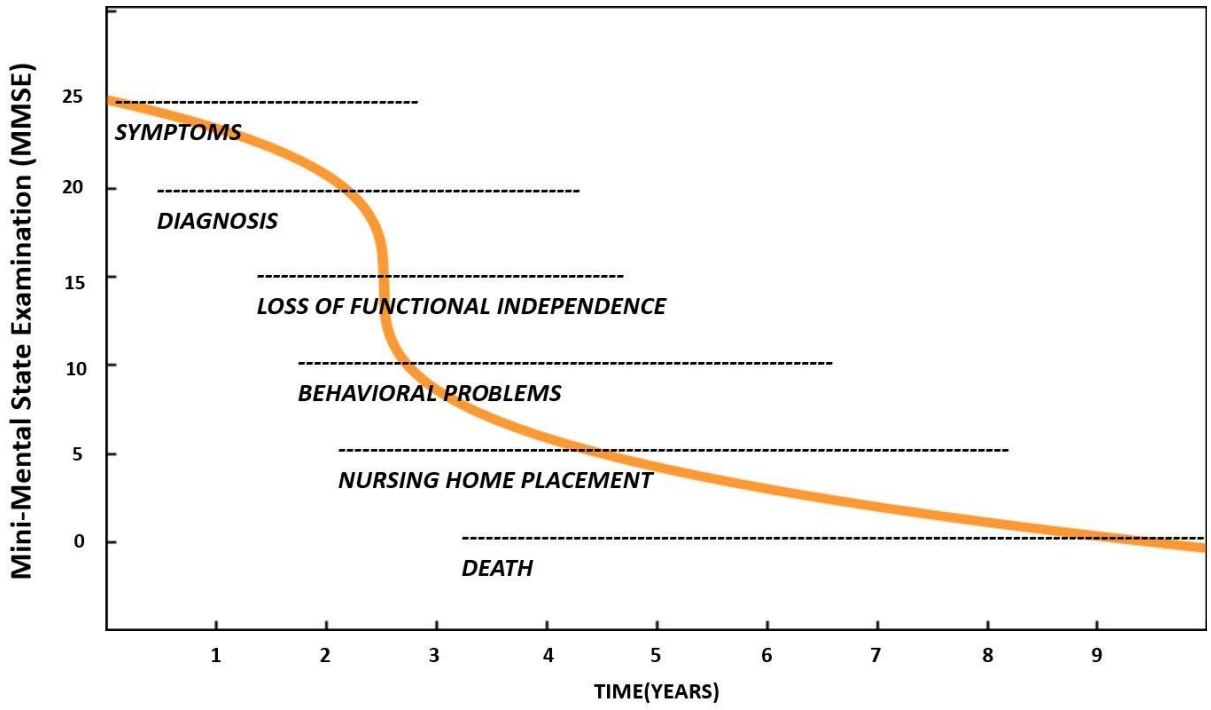

Figure 1.2 Natural history of Alzheimer's disease. Adapted from Feldman and Gracon, 1996.

Using neuroimaging to compare differences in cognitive function between AD patients and healthy individuals provides the opportunity to better understand the progression of the disease. Neuroimaging for AD also provides the opportunity to improve early detection based on identified differences between AD patients and healthy individuals.

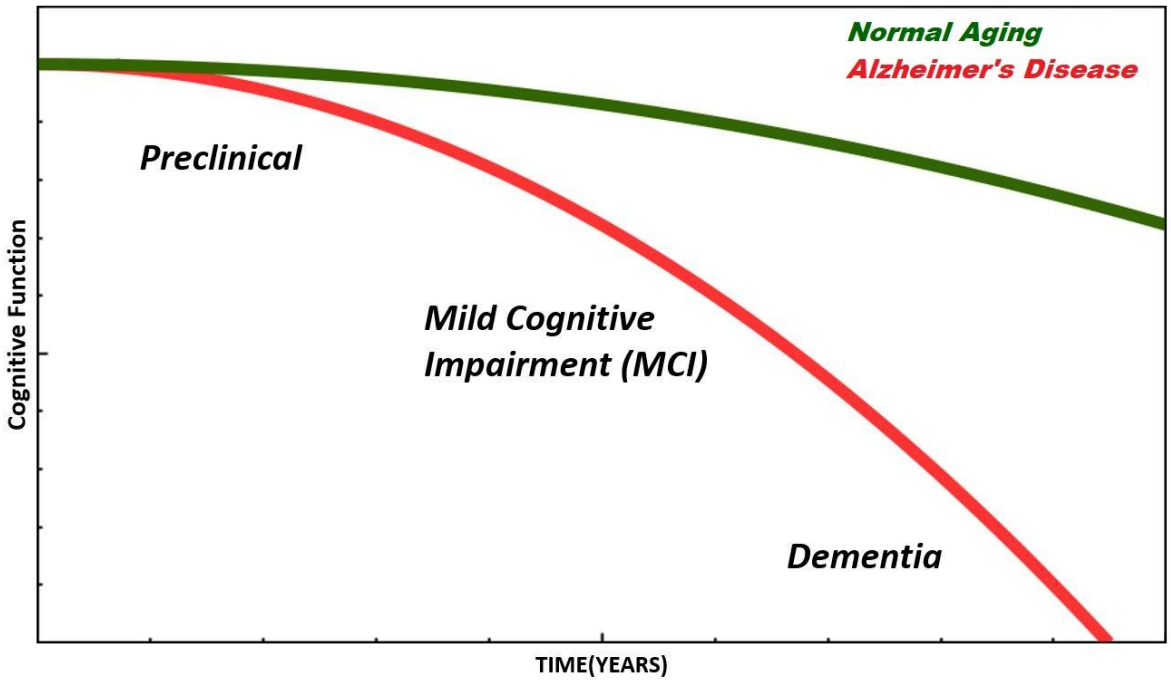

Figure 1.3 Three stage progress of Alzheimer's disease.

Currently, various methods in neuroimaging are being used for the detection of AD. Positron emission tomography (PET), magnetic resonance imaging (MRI), and functional MRI (fMRI) are common neuroimaging methods that have been widely used to study AD. PET is a neuroimaging method used for detecting changes in metabolic activity in the brain. The disadvantages of the PET technique include its use of radioactive substances and its low spatial and temporal resolution.

MRI is a neuroimaging method used to generate images of organs in the body. MRI uses protons and electromagnetic waves to obtain images with high spatial resolution. MRI does not have any known side effects and is therefore widely used in clinical imaging. The fMRI method is a dynamic version of MRI and is widely used to study human brain function. Some of the advantages of fMRI include the use of non-ionizing radiation, the ability to be non-invasive, the capacity to efficiently scan a single patient multiple times, and adequate spatial

and temporal resolution (Bi et al., 2018, Tepmongkol et al., 2019, Giffard et al., 2008, Li et al., 2002).

Resting-state functional magnetic resonance imaging (rs-fMRI) is becoming more popular in the field of neuroimaging. For patients with AD, rs-fMRI is emerging as a standardized method which allows for the measurement of functional connectivity in the brain. The use of rs-fMRI suggests that data or model-driven methods can enable researchers to discern the decline of brain function. More information regarding fMRI is discussed in Chapter 2.

1.2 Biomarkers

Biomarkers, first created for chronic pain disorders, are measurable parameters that can be used to reliably identify disorders. Examples of biomarkers used today include prognostic and predictive markers which, as the name suggests, can determine the risk of future pain and ascertain the effects of treatment (van der Miesen et al., 2019, Woo & Wagner, 2015). Neuroimaging biomarkers have certain features that can classify biomarkers as functional or not. In the field of AD, technological advances have been made in identifying biomarkers by using neuroimaging approaches to recognize changes that are associated with the progression of the disease, especially in the frontal gyrus (FG) and the default mode network (DMN). In AD patients, functional connectivity between the FG and other brain regions appear abnormal, which may explain memory dysfunction and allow FG to be a potential biomarker for AD (Bi et al., 2018). Suitable biomarkers must provide reliable information about the condition of the living organism, and effective biomarkers are those that can allow us to better understand a condition. This means that a biomarker should have distinguishable parameter(s) that are able to identify significant differences and distinct conditions. A quality biomarker should offer accurate diagnostic performance in classification or prediction of the condition, which is

accomplished based on the sensitivity of the technique (Damoiseaux, 2012, Woo et al., 2017, Woo & Wagner, 2015).

1.3 Objectives

The objective of this study is to see if the progression of Alzheimer‘s disease can be explained by applying a multiple linear regression analysis using the information from ReHo and RSFC spatial maps, and determine if this information can be used for early detection for this disease. Altered brain regions in AD patients were determined by using several complimentary approaches such as independent component analysis (ICA), regional homogeneity (ReHo), and amplitude of low-frequency fluctuations (ALFF). Spatial maps, generated from rs-fMRI scans of AD patients and HCs and analyzed using a multiple linear regression analysis, are to be used to compare the two groups in a longitudinal approach. In this study, three regions were selected to be used in multiple analysis techniques using age and condition (HC or AD) to separate the two groups and identify the progression of the disease. Chapter 4 explains the various analysis methods used for this study in more detail.

1.4 Outline

The outline of this thesis is presented as follows: Chapter 1 – Introduction, Chapter 2 – Magnetic Resonance Imaging and Data Acquisition, Chapter 3 – Image Processing Methods, Chapter 4 – Functional Connectivity and Statistical Analysis, Chapter 5 – Results, Chapter 6 – Conclusion and Discussion.

CHAPTER 2

MAGNETIC RESONANCE IMAGE SCANNING AND DATA ACQUISITION

2.1 Magnetic Resonance Imaging Techniques

2.1.1 Magnetic Resonance Imaging Review

Magnetic Resonance Imaging (MRI) uses large magnetic fields with radiofrequency signals in conjunction with hydrogen protons in our body to create high resolution structural images of soft tissue. MRI has been used to study structural brain differences between healthy controls and diseased patients, such as AD patients. fMRI has been used during both stimulus/task activation and during the resting state condition to study systems-level human brain function. In this section, MRI and functional MRI will be introduced to provide a background for the techniques used in this study.

MRI uses strong magnetic fields in conjunction with radiofrequency signals at preset frequencies (Larmor Frequency) to generate images. The generated magnetic field strengths are typically represented in tesla (T), where one tesla equals 10,000 gausses. Although 3T machines are widely used for human research, there are also 1.5T, 7T, and 11T MRI scanners available. An MRI scanner has three main components, each represented by a letter in the MRI acronym. The letter M in MRI stands for magnetic fields, which are typically generated by superconducting coils within the machine. The magnetic field is responsible for stimulating hydrogen protons or spin vectors. Stimulated spin vectors all align in the same direction of the magnetic field. The letter R in MRI stands for resonance, which is the delivery of radio frequencies (RF) at the Larmor frequency. The Larmor frequency is the frequency value needed to stimulate aligned spin vectors in a given region. In other words, the Larmor frequency is the frequency value of the atomic nuclei for a hydrogen atom at a particular magnetic amplitude. Lastly, the letter I in MRI stands for imaging. Imaging for an MRI scanner requires an alteration

of the magnetic field strength over space. This can be done by turning the coils on and off. Acquired signals are used within Discrete Signal Processing (DSP) cards to reconstruct the incoming signals from the X – Y – Z planes to create a 3D image of the target tissue that is being scanned (Huettel et al., 2014).

MRI scanners use pulse sequences to control the timing of signal excitation and data collection and to generate images from biological tissues. The pulse sequence is a feature that allows an MRI scanner to acquire images with distinct timing to highlight different tissues with different physical properties. By using different pulse sequences, it is possible to create images of different biological tissues (bones, tumors, muscles). However, MRI has several limitations, such as difficulties in scanning patients with claustrophobia, obesity, and/or metal implants (Huettel et al., 2014). In spite of these limitations, MRI is routinely used for clinical imaging and remains one of the most popular methods for performing structural imaging.

T1 and T2 relaxation times are used as a means of generating images for brain mapping. T1 relaxation is used for anatomical images and is the most common technique used to generate 3D structural images of the brain. Anatomical images are also known to be called T1 images if T1 relaxation is used during generation. T1 relaxation, or T1 recovery time, is the amount of time spent for a spin vector to get its maximum longitudinal magnetization value after an RF pulse. In other words, the T1 recovery graph is the longitudinal magnetization value as a function of time after an RF pulse.

T2 or T2 decay graphs are generated similarly. However, T2 uses the transverse magnetization value as a function of time. Another value that is important in T2 decay graphs is T2*. T2* is the decaying sinusoidal signal used in fMRI. Using the T2-weighted MRI technique, manipulations in blood oxygen can be measured (Ogawa et al., 1990). The gradient echo approach is often used with different variations to make tissues sensitive to T2* contrast. T2* can produce blood origination dependent changes and is always shorter than T2. In

summary, the T2* principle is the foundation for a BOLD contrast. It is the main reason that fMRI has a high temporal resolution (Huettel et al., 2014).

2.1.2 Functional Magnetic Resonance Imaging Review

The term fMRI, as the name implies, allows us to investigate human brain function for a short time period. The data is typically sampled every 2 seconds, referred as the repetition time (TR). fMRI has a high temporal resolution that can measure short-term functional activity changes, allowing researchers to localize brain activity on a second-by-second basis. Since fMRI also has high spatial resolution capabilities, fMRI is a powerful tool to investigate brain activity. Unlike PET, fMRI does not use radiation or isotopes and is non-invasive, allowing patients to be scanned multiple times. These features are the main reason that made fMRI a popular investigative tool. Currently, fMRI is one of the most essential and standard investigative neuroimaging tools that many researchers prefer to use.

fMRI uses Blood Oxygen Level Dependent (BOLD) signal changes to measure functional activity (Huettel et al., 2014). The blood oxygen level dependent (BOLD) signal, which is detected with fMRI, shows the changes in deoxyhemoglobin with localized changes of brain blood flow and blood oxygenation. This shows the underlying neuronal activity by presuming more oxygen will be used in more active parts of the brain in a mechanism known as neuro-coupling. There are mainly two kinds of fMRI techniques that are performed: task-based fMRI (task-fMRI) and resting-state fMRI (rs-fMRI). As the name suggests, task-based fMRI uses various tasks during the scanning procedure. In task-based studies, a stimulus/task is presented for a short period of time alternating with periods of control conditions. It is currently believed that when a subject performs or responds to a task, there is an increase in neuronal firing in specific regions of the brain. These increased neuronal firings result in an increased consumption of blood oxygenation, leading to vasodilation. The increased blood flow

results in more oxygenated red blood cells than is needed, and the difference between oxygenated red blood cells and deoxygenated red blood cells results in signal increases in regions associated with the task. On the other hand, rs-fMRI checks for functional activity in the brain while the subject is resting. In other words, no specific task scans are acquired in rs-fMRI, and the subjects are simply instructed to rest (Huettel et al., 2014, Purves et al, 2011, Heeger & Ress, 2002).

In terms of rs-fMRI, functional connectivity refers to the synchronization of brain regions that can form resting-state networks. In other words, functional connectivity is the common activity of spatially separated regions of the brain. These regions that have common or synchronized activity create resting state networks such as Default Mode Network, Medical Visual, Medial Temporal, etc. With this technique, it is possible to identify linked locations within the brain without the need for a physical connection between the brain regions. Usually, fMRI images have a 3 mm spatial resolution. This value is lower than T1 images. Furthermore, fMRI images are overlaid on the T1 images to help with the identification of brain regions in terms of structure (Lee et al., 2013).

Although MRI and fMRI both use the same principles and the same scanner, they are not the same. The main difference between fMRI and MRI for neuroimaging is that fMRI provides information about functional activity in the brain as a function of time. In contrast, MRI provides structural information about the brain. In other words, MRI scans provide anatomical scans of the brain, while fMRI scans provide information on the metabolic function of the brain (Huettel et al., 2014). Furthermore, fMRI provides functional information about the brain as well as how, when, and where a particular brain function occurred. It can also link various brain networks and their relation, or functional connectivity, with other networks.

2.1.3 Blood Oxygen Level Dependent (BOLD) Signals

Increased metabolic activity in a brain region, as reflected in an fMRI scan, implies that neurons in that region are active. Active neurons use more energy to be able to do their work, and more energy means more oxygen consumption. For neurons to be able to consume more oxygen for energy, there needs to be more oxygen in the area. Therefore, the need for oxygen to be used for energy affects neighboring blood vessels in the region to create increased oxygenated blood flow to that region. In summary, when there is increased metabolic activity at a brain region, the amount of blood flow increases as a result of glucose breakdown (Ogawa et al., 1990, Biswal et al., 1997, Huettel et al., 2014).

Deoxygenated blood is visible with gradient-echo imaging. Gradient echo imaging uses free induction decay (FID) signals. FID is a short-lived sinusoidal signal that comes from the spin vectors after a 90-degree radiofrequency pulse. Every tissue characteristic of the FID signal will be different; thus, the incoming signal will be different. Differences in FID signals allow for the separation of different tissue types from each other. In summary, deoxygenated blood is a natural contrast that can be visualized with gradient-echo imaging using MRI. The concept used in FID signals also led to the creation of the concept of the BOLD signal (Ogawa et al., 1990, Huettel et al., 2014). The BOLD signal is a metabolic signal, and changes in the ratio of oxyhemoglobin to deoxyhemoglobin are measured and can be linked to changes in neural activity (Azeez, 2019, Ogawa et al., 1990).

The response of a neuron is much faster than the BOLD signal itself. Although indirectly, the BOLD signal response effect is from the firing of nerve cells. The hemodynamic response function (HRF) explains the changes in cerebral blood flow, oxygenation, and volume. BOLD signals are defined using HRF with fMRI. In other words, oxygenated blood gets converted to deoxygenated blood. Moreover, when neurons become active (when neuronal firing occurs), blood flow increases and results in increased oxygenated blood to that location.

This process leads to a high-intensity response from the location of the scanned area that can be seen with fMRI (Ogawa et al., 1990, Boynton et al., 1996, Cohen, 1997).

BOLD signal contrast depends on the amount of blood with deoxygenated hemoglobin, which will consume the present oxygen, within the brain region. The changes that happen in the BOLD signal are called HRF, and the fMRI modality is based on that principle. The BOLD signal can be seen with task-based fMRI research. Task-based fMRI (task-fMRI) is where subjects perform specific tasks during the fMRI scan, like finger tapping. Resting-State fMRI (rs-fMRI) checks for neurologic processes that occur without the need for tasks and, unlike task-fMRI, does not limit the experimental design or the number of questions that can be answered with the technique (Azeez, 2019, Huettel et al., 2014).

Furthermore, fMRI has a high temporal resolution, which is around 500 milliseconds to 3000 milliseconds (ms). Generally, a stimulus takes about 10 seconds, enough to able to see the neuronal activation as a function of HRF. A temporal resolution of 500 to 3000 ms (TR value) is good enough to answer most research questions. In resting state, frequency characteristics of neuronal activity within the BOLD signal can be seen under 0.1 Hz. However, the BOLD signal has components both above and below 0.1 Hz. The effects of respiratory and cardiac response on the BOLD signal can be seen in frequency values higher than 0.1 Hz. Generally, the elimination of these non-neuronal effects from the BOLD signal in rs-fMRI studies is needed. Therefore, band pass filtering is typically used. Generally, the low cutoff frequency equals to 0.01 Hz (to eliminate small frequency noise from various sources) and the high cutoff frequency value is 0.1 Hz, as mentioned earlier (Biswal et al., 1995, Glover, 2011). The reduction of noise and removal of non-neuronal signals in this study will be explained in more detail within Chapter 3.

2.1.4 Application of Functional Magnetic Resonance Imaging

Neuroimaging has had a crucial role in AD studies for the past four decades with different modalities such as computed tomography or MRI. More recently, structural and functional MRI showed significant changes in the brains of AD patients. No single neuroimaging modality can produce every possible image of other neuroimaging techniques, but they all have their uses and weaknesses. With AD, it is not always clear to make a clinical diagnosis without the use of neuroimaging; for a definitive diagnosis, neuroimaging is needed (Smitha et al., 2017).

In terms of structural imaging, MRI can detect progressing atrophy (volume), and the brains of AD patients can have vascular damage that will alter incoming MRI signals for the T2 images for some sequences. Progression of AD can be identified by checking cerebral atrophy in the brain, which starts early in AD. Atrophy first manifests itself in the medial temporal lobe, which is the first sign of AD. Because of this, atrophy of the medial temporal lobe is considered to be one of the biomarkers in AD that can be detected with structural MRI (Johnson et al., 2012, Smitha et al., 2017).

In terms of functional imaging, fMRI is a fairly new method when compared to structural MRI. Brain networks related with memory and other cognitive functions of AD patients are getting increasingly investigated with fMRI. Both task-fMRI and rs-fMRI give information about functional connectivity within the brain networks of an AD patient and can be useful in early detection of AD. Although fMRI has potential for this, a relatively smaller number of studies are published that are made with AD patients. There are some studies that reported a decrease in the medial temporal lobe in patients with mild cognitive impairment (MCI). Recently there is some increase on studies with BOLD fMRI techniques and spontaneous brain activity with rs-fMRI on AD patients. Especially in terms of pharmacology, fMRI might be the best way to monitor cognitive function in AD patients. Furthermore, longitudinal studies are needed to make sense of the fMRI activation patterns. Currently, the

focus is on characterization of vascular and metabolic features in brains of patients with AD (Lajoie et al., 2017, Johnson et al., 2012, Smitha et al., 2017).

2.1.5 Limitations of fMRI

The temporal resolution in fMRI, which can be achieved by the high scanning speed of the modality, needs larger voxel sizes to maintain the required level of signal to noise ratio (SNR). For this reason, fMRI has increased temporal resolution and decreased spatial resolution from the generated images. The limit for temporal resolution in fMRI is set by the BOLD signal. As it is not possible to increase the speed of neuronal responses, and BOLD signals are generated from the neuronal responses, maximum temporal resolution is dependent on the BOLD signal (Huettel et al., 2014, Poldrack et al., 2011).

One of the significant challenges of fMRI is head motion during the scan. Patients often move during scanning, and in most cases the patient's head motion during the scan cannot be avoided. This issue would be a huge problem since AD patients might have conditions that may make them less compliant, such as mood swings or short-term memory problems. Because of the compliance issues, head motion effects would be problematic for both rs-fMRI and task-fMRI. However, there are methods to be used during the scan and algorithms in pre-processing steps that can eliminate the effects of head motion. In some cases, head motion can be corrected for after pre-processing fMRI images, allowing further analysis to be performed (Huettel et al., 2014, Poldrack et al., 2011).

In fMRI, like PET, patients with claustrophobia may face challenges, since fMRI imaging requires patients to be in a tight and enclosed space during the scanning time. fMRI is based on magnetic force, so patients with metal implants or some metal-based tattoos cannot be scanned with fMRI, thereby presenting an additional limitation to the use of fMRI as a neuroimaging technique. This also applies for some patients with pacemakers (Basil et al.,

2018). Lately, there are productions of MRI compatible pacemakers that will enable patients with these pacemakers to be allowed for fMRI scans. Also, patients with obesity may not be compatible for fMRI if their measurements are more than what the machine can handle (Huettel et al., 2014, Poldrack et al., 2011).

Lastly, the scan time is another factor that limits fMRI studies. Generally, a fMRI scan takes between 2-12 minutes. Individual time points are not independent in terms of statistics in BOLD signals. Since they are not statistically independent for each fMRI scan, the correlation value must be corrected for degrees of freedom to determine significance. In short scans, estimating significance becomes problematic because of a low number of time points available. To fix this issue, scanning time higher than 5 minutes is needed to allow detection of most studied networks such as the default mode network. Furthermore, increasing the time decreases the noise and increases the correlation strength, but may not be necessary. Increasing the scanning time might cause more head motion or discomfort to the patient so the optimal scanning time of 5-6 minutes appears to be sufficient for most studies (Van Dijk et al., 2010).

2.2 Data Acquisition

This study was performed on a public dataset from "Alzheimer's Disease Neuroimaging Initiative" (http://adni.loni.usc.edu/). MRI and fMRI techniques were used to acquire anatomical and functional images for each subject. The subjects of this study included both healthy controls and patients with Alzheimer's disease. T1-weighted images were acquired using both 1.5T and 3T MRI scanners at different sites and the spatial resolutions of the anatomical images were 1x1x1.2 mm^3. All fMRI images were acquired with 3T Philips MRI scanners. Parameters of fMRI scans: TR (repetition time) = 3000 ms, TE (echo time) = 30 ms, flip angle = 80^o, matrix = 64 x 64, slices =15 and, voxel size = 3.3125x3.3125x3.313 mm^3. There were 140 time points for each scan and length of the scans were 7 min long. With the

fMRI scans date-time of the scan, age of the subject, condition of the subject (Healthy Control or Alzheimer's disease patient), and sex information were available this dataset. As reflected in the public data set, there were different numbers of scans for each subject acquired at different dates.

CHAPTER 3

PRE-PROCESSING METHODS

In this section, the pre-processing methods are described with a focus on the methods used in the current study. Additionally, the definitions of each of these processes and the importance of these functions are presented. fMRI applies a series of set algorithms on the obtained dataset. In this model, it is often necessary to eliminate white noise in the data to improve the signal to noise ratio. The process of eliminating noise and unnecessary data from CSF and large ventricles is regarded as pre-processing. Also, the fMRI data is transformed to a standardized space to make the comparison between 2 or more brain scans possible. The pre-processing pipeline may differ for each study but is generally initiated with the realignment of the functional images.

During this phase, additional steps are often needed before realignment depending on the dataset. These can include reorienting functional and anatomical images. The pre-processing pipeline of realignment, coregistration, segmentation, normalization, temporal regression, and filtration is applied across all the subjects within the dataset. To increase the efficiency of pre-processing, scripts are provided in standard software programs, which can be run in a batch from the Statistical Parametric Mapping software SPM12 (Friston et al., 1994) in MATLAB (Higham & Higham, 2016). AFNI (Cox, 1996) and MATLAB were used in this study for both pre-processing and data analysis. To provide a more comprehensive review of pre-processing, the following sections will discuss the individual steps.

Pre-processing steps. In this section, the steps taken before statistical analysis is presented. Pre-processing is applied to make sure all the data is in the same orientation, corrected for head motion-induced signal changes, and transformed into the MNI space for future statistical

analysis. These steps are required to achieve statistically significant results. In this study, the pre-processing is carried out as follows:

1. Realignment of functional images,
2. Coregistration of functional images to anatomical images,
3. Segmentation of the anatomical images,
4. Normalization of functional images to the MNI space from subject space,
5. Creation of tissue masks from segmented files of anatomical images,
6. Extraction of information from white matter (WM) and cerebral spinal fluid (CSF),
7. Temporal regression using motion parameters and information form WM and CSF, and
8. Bandpass filtration of signals to 0.01 – 0.1 Hz band.

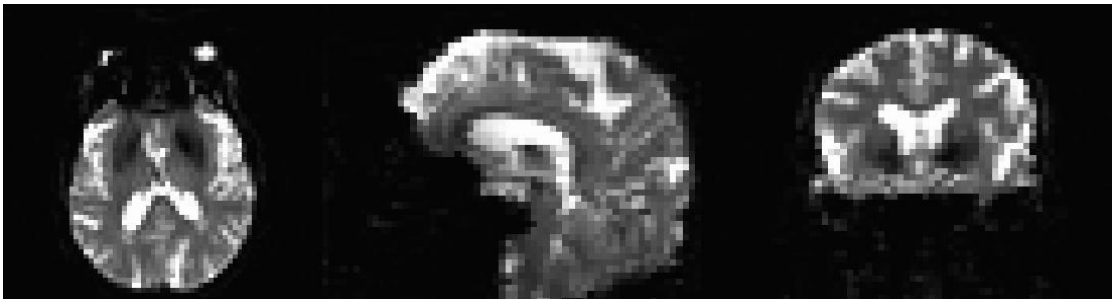

Figure 3.1 Raw fMRI image of an anonymous subject from the current study in the native space (left to right: axial – sagittal – coronal view).

Source: http://adni.loni.usc.edu/.

3.1 Realignment

The first step of pre-processing is realignment. Realignment step is standard step for fMRI images to minimize the effects of head motion. This process is necessary as it is not possible to ensure complete stillness during the scanning process. However, patient movement can produce false-positive results within the fMRI data of that subject. Realignment attempts to align all the time points in a fMRI time series. This is necessary because some of the time points in an image time-series may not have a proper alignment to a reference image, and the reference image

could be any of the time points within a functional scan or the mean of all the time points within a scan (Hafiz, 2017). Thus, all the images must align with each other to ensure all errors are corrected for in the final analysis (Friston et al., 1996, Poldrack et al., 2011).

For this process, the motion correction algorithm uses a least-squares method with a six-parameter rigid body transformation (Friston et al., 1995) representing three rotational (pitch, roll, yaw) and three translation (x, y, z) parameters. In realignment, a file with information on these six parameters is generated to further minimize any motion-related artifacts (Hafiz, 2017). After realignment, the images are resliced such that they match the first image selected voxel-for-voxel to deal with signal discrepancies before normalization. The realignment for this study has been performed using SPM12.

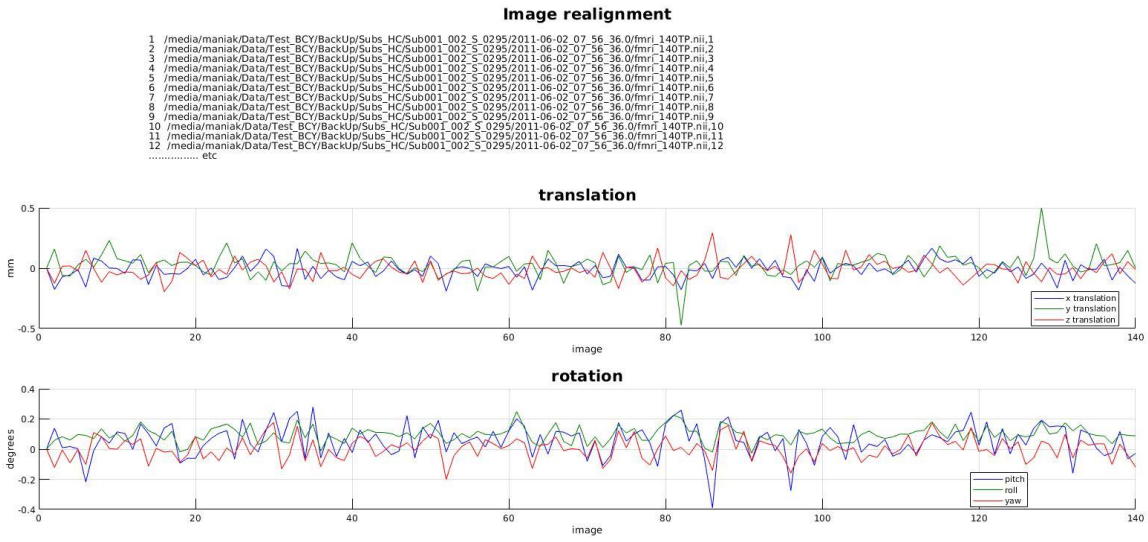

Figure 3.2 Realignment output of a single fMRI scan from the study

3.2 Coregistration

The coregistration process consists of aligning and overlaying the fMRI data on the anatomical image. To be able to use these images together, they need to have the same coordination with each other. Coregistration is used to align the head-motion-corrected fMRI images towards the inputted anatomical images to ensure the alignment of anatomical and fMRI images. In other

words, the corrected images are aligned with the anatomical image to allow for an accurate spatial fit.

The main reason for registering fMRI images to anatomical images is to allow SPM12 to identify the regions of the brain since anatomical images have much better spatial resolution. Furthermore, the high-resolution quality of anatomical images increases efficacy for assessing brain locations of fMRI scans of each brain. Through coregistration, viewing the functional information regarding the brain is improved due to the correlation with anatomical and high-quality spatial data. As such, this model was also employed in this study.

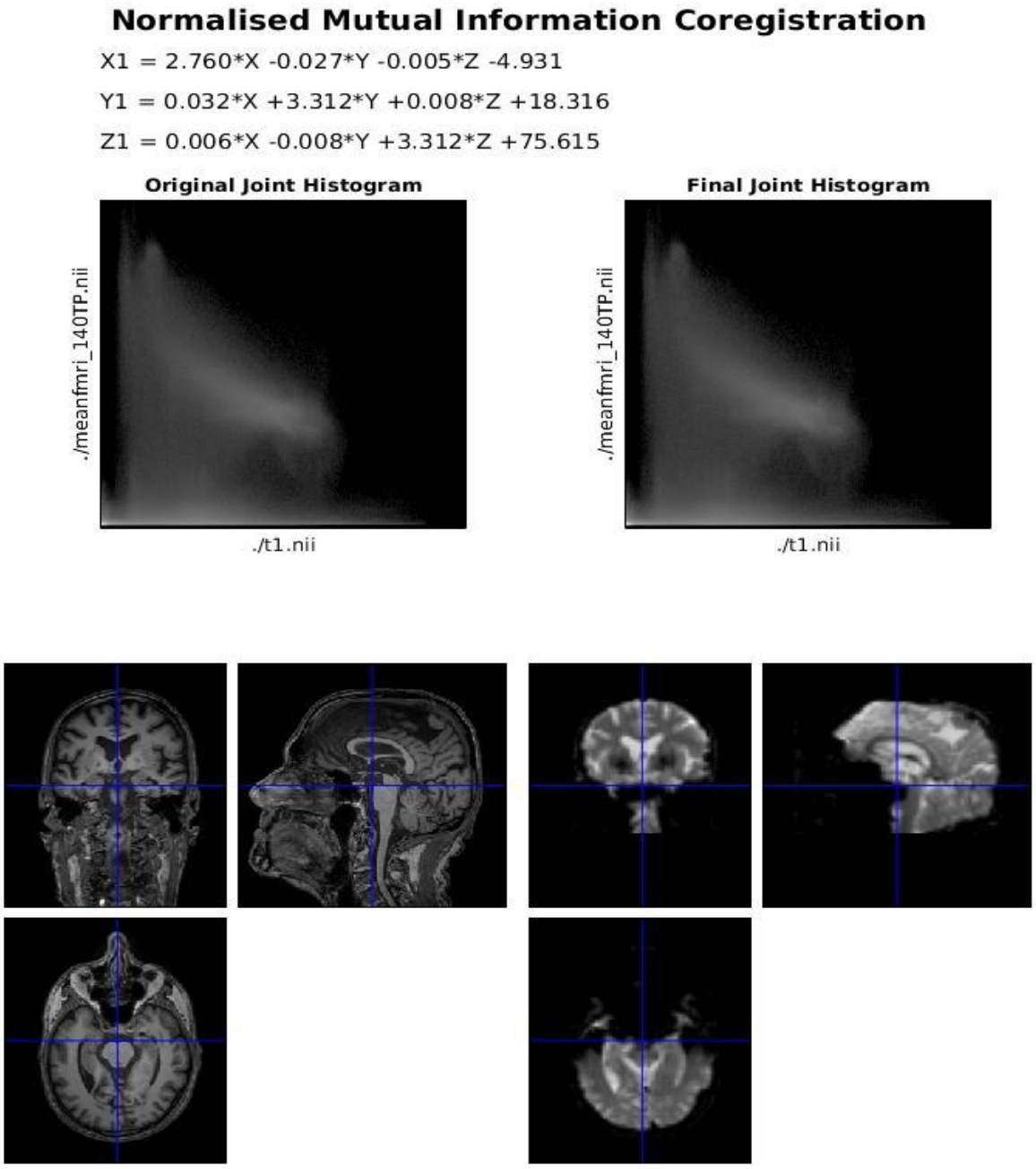

Figure 3.3 Coregistration output of a single fMRI scan from the study.

Source: http://adni.loni.usc.edu/.

3.3 Segmentation

After coregistration is complete, the next step in the pre-processing pipeline is segmentation. Segmentation is the process that partitions the anatomical (or functional) image into different tissue classes. Segmentation is critical due to the integral human brain anatomy. The human brain is classified within three different tissue types, (1) gray matter (GM), (2) white matter (WM), and (3) cerebrospinal fluid (CSF). Thus, segmentation is critical to ensure that the anatomical skull categorizes the separation of the brain tissue. Each anatomical brain image is used for each patient. Figures 3.4 and 3.5 illustrate the process of segmentation for this study.

In this process, intensity differences in the anatomical MRI images are used. When using SPM12, a series of 6 differing tissue types are generated. These tissues are GM, WM, CSF, skull, soft tissue, and remaining parts of the scan (the outside region). It is also essential to consider the bias information. In this model, bias field estimation and correction is the normalization of values for different tissue types in the brain. Correction for the inhomogeneities dramatically increases the accuracy of the segmentation process. SPM12 does all of this in a single step. WM and CSF tissue classes are used to generate masks for further steps along the pre-processing pipeline.

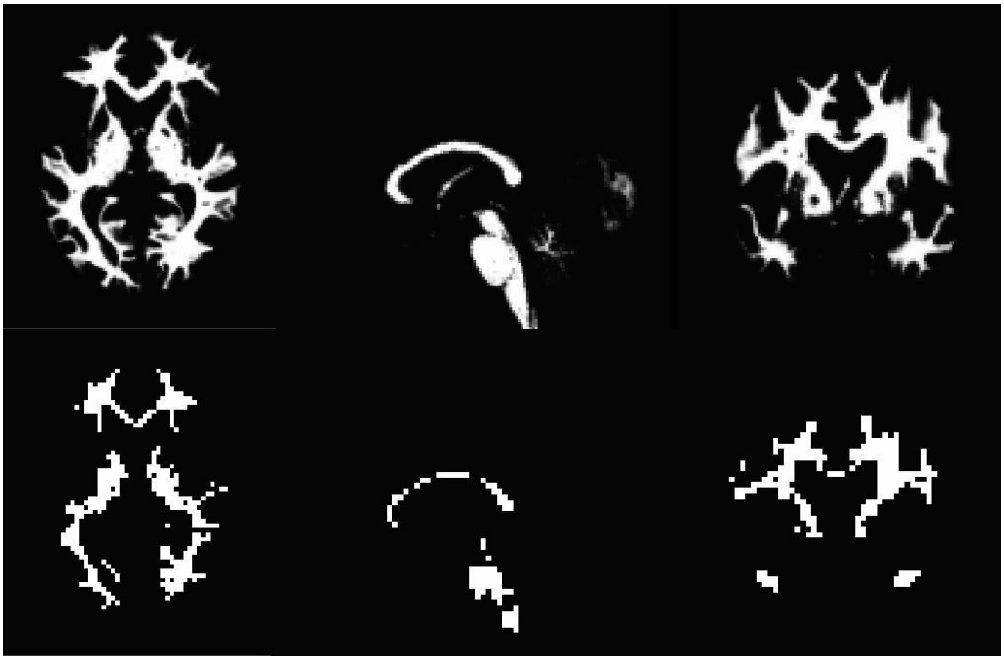

Figure 3.4 White matter output of segmentation of a single anatomical scan from the study in MNI space (top) & generated mask using 0.98 as the threshold value (bottom).

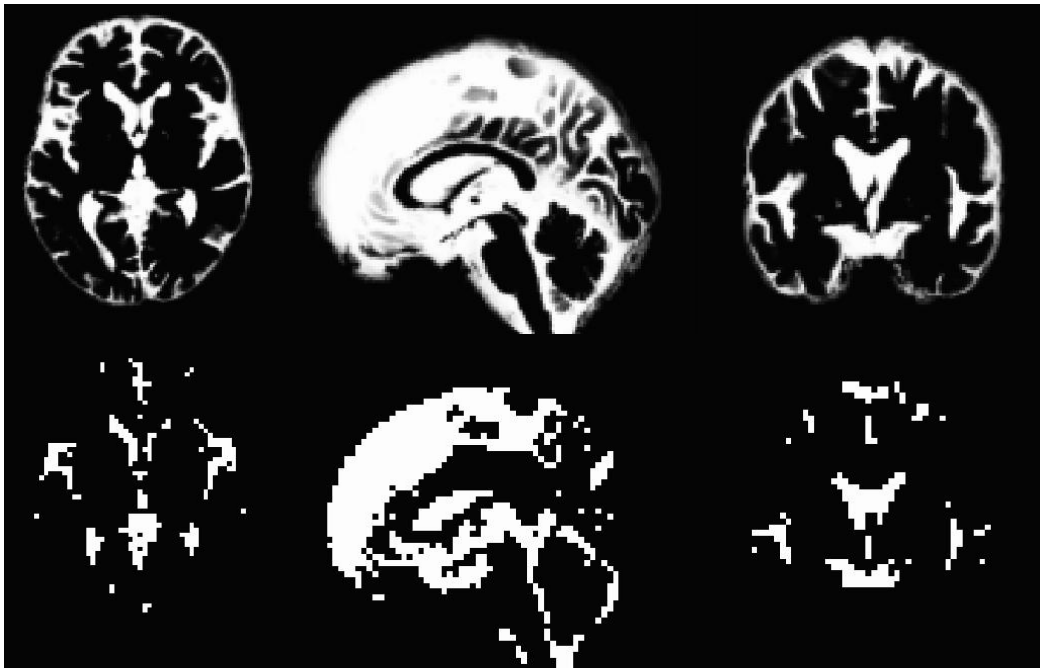

Figure 3.5 Cerebral spinal fluid output of segmentation of a single anatomical scan from the study in MNI space (Top) & generated mask using 0.98 as the threshold value (bottom).

3.4 Normalization

The process of normalization includes transforming every image into a generic template, such as the MNI template, that can be applied to all fMRI images. In this process, images from each of the subjects are transformed into a standardized space so that all images for every subject will have the same coordinate system and can be processed for statistical analysis. This step is vital for group-level analysis. As mentioned earlier, all functional images are in their native space, and every native space is different from that of other native spaces. Thus, each patient's brain size and shapes are different, and it is necessary to ensure that these different shapes are in a normalized space for future analysis. For batched or group-level analysis, images must be in a standard space. The process of normalization warps each patient's brain size and shape into a standardized brain model that ensures that the spatial fit of all brains are the same. Thus, the coordinates for comparison between brains is possible through this process of normalization. The most common standardized space templates are the Montreal Neurological Institute (MNI) space and the Talairach Space.

For this study, the MNI152 space was used for transformation (figure 3.6). The MNI152 template was created from 152 brain scans of a young adult. SPM12 requires both anatomical images and fMRI images of each patient to perform transformation of images from native space to MNI152 space.

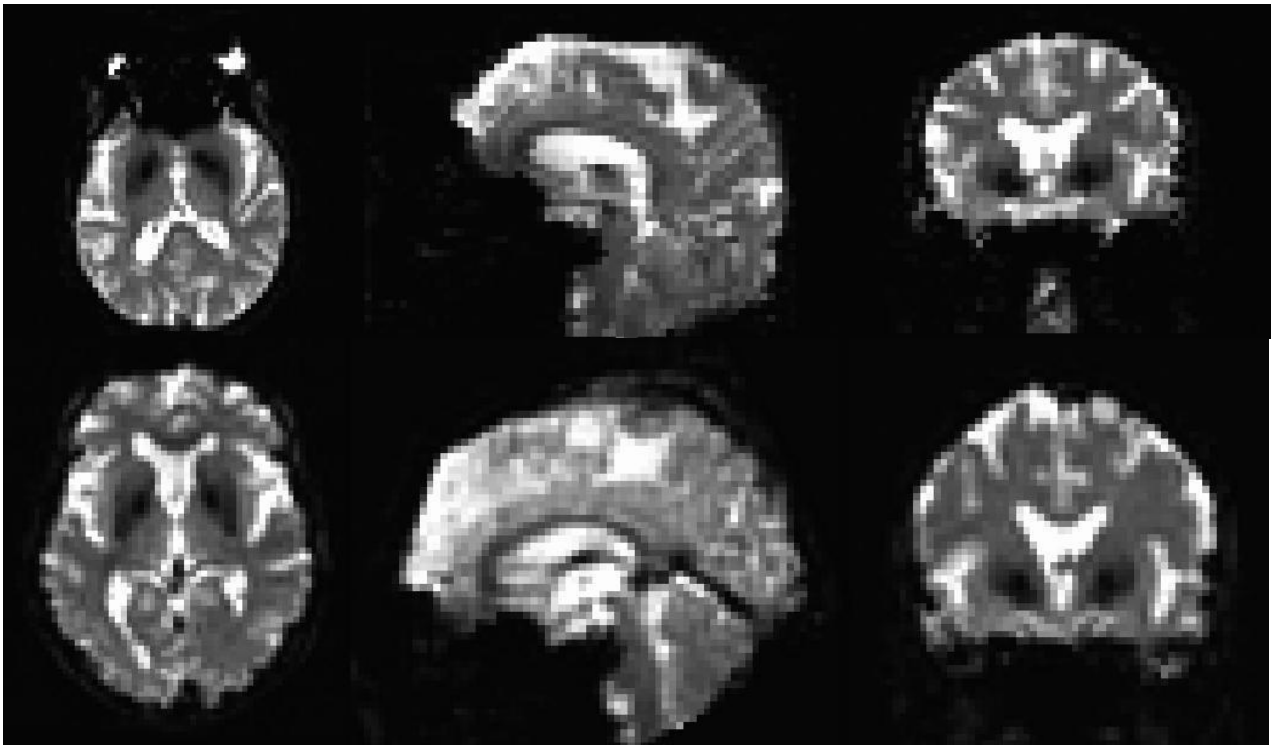

Figure 3.6 Differences between outputs after coregistration (top) and normalization (bottom) of a single scan from the study into MNI space.

3.5 Nuisance Regression and Temporal Filtering

For this study, PCA was used for assessing correlated components within the fMRI data to perform nuisance regression. PCA also assesses voxels synced with each other in specific regions within the fMRI data. Thus, the principal components or eigenvectors (e.g., a value different than zero) of the covariance matrix of the fMRI data was identified. After the normalization step in the pre-processing pipeline, WM and CSF images from segmentation are used to create masks. The masks were generated using 0.98 threshold values of the segmented images of WM and CSF and resampled to the voxel size of the functional images. A PCA of 5th degree was run on the fMRI data using the respective WM and CSF mask for each individual subject. Doing this allowed synced voxels within WM and CSF in the brain regions to be gathered in a single covariance matrix. These generated values include data from the WM and CSF regions, and since the point of interest is the data from GM, linear regression of these generated WM and CSF values were made in the regression step. This would allow exclusion

of the effects of WM and CSF that we would see from the group analysis of the data. PCA had been done on the functional scans with MATLAB to be used in the temporal regression step (Hafiz, 2017).

As noted, regression is used to get rid of effects from WM and CSF. Furthermore, motion parameters from the realignment step were also regressed out from the fMRI scans. Both extracted values from PCA and 24 motion parameters (six motion parameters, derivatives of each motion parameter, forward derivatives of each motion parameter, as well as squared forward derivatives of each motion parameter) were used in the regression step. In other words, a total of 34 regressors were used in the regression step. To regress out these 34 regressors from the fMRI scans, MATLAB was used. First, ten time-points of the time series of the fMRI scans were removed to avoid false-positive results, which can be caused by the scanning process's adaptation period at the start of the procedure (Azeez & Biswal, 2017, Hafiz, 2017). After temporal regression, a bandpass temporal filter in the range of 0.01-0.1Hz was applied to all time series, to remove any physiological noise and other artifacts using AFNI. This is a standard process for rs-fMRI research (Biswal et al., 1995, Hafiz, 2017).

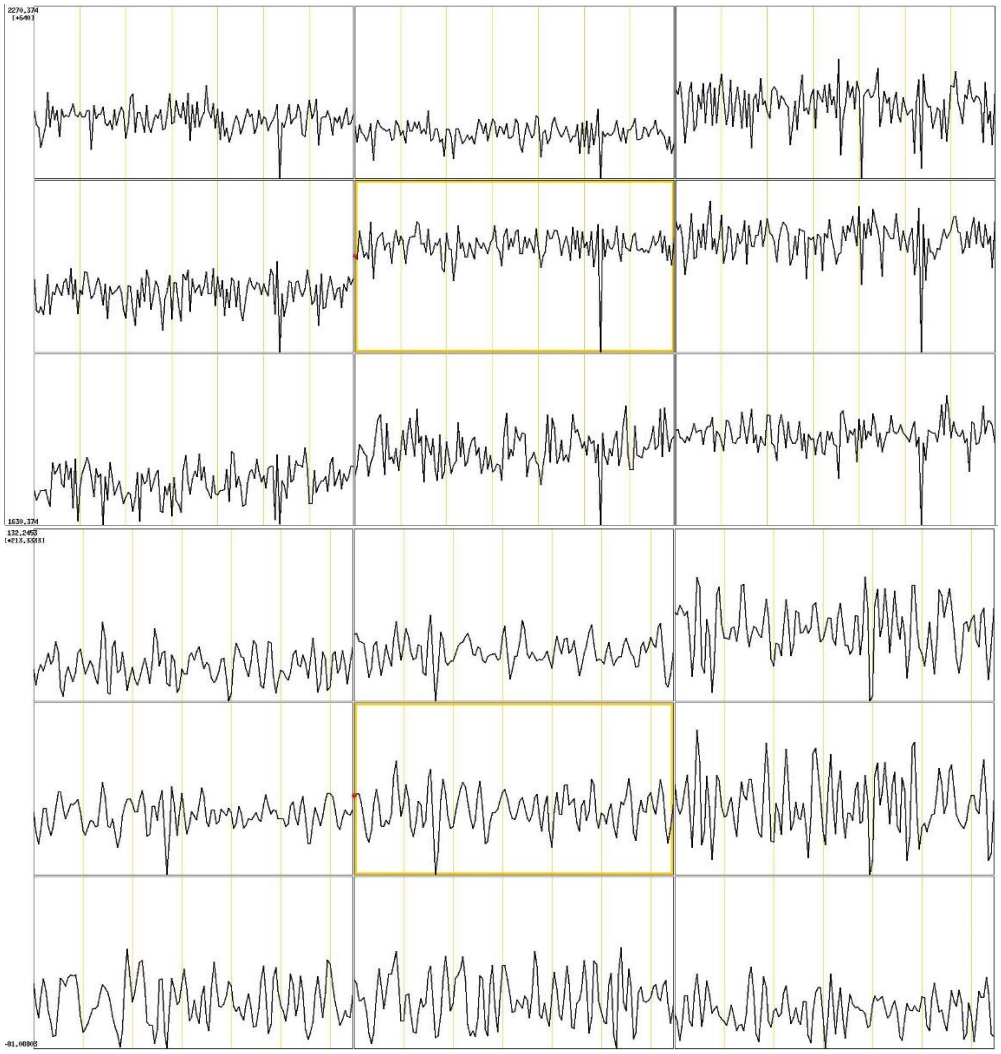

Figure 3.7 Signal differences in the hippocampus between normalized fMRI image (top 9 graphs) & filtered and regressed fMRI image (bottom 9 Graphs) for a single fMRI scan from the study.

3.6 Smoothing

For the last step of pre-processing, spatial smoothing was used to increase the signal to noise to noise ratio. A 6mm full width at half maximum (FWHM) filter was used for smoothing. The 6 mm FWHM was used because the voxel size of the normalized fMRI images was 3mm. For best results, twice the voxel size number of the fMRI image must be used as the FWHM value. Also, for certain data sets with enough samples, it is crucial to use a minimum FWHM value (Poldrack et al., 2011).

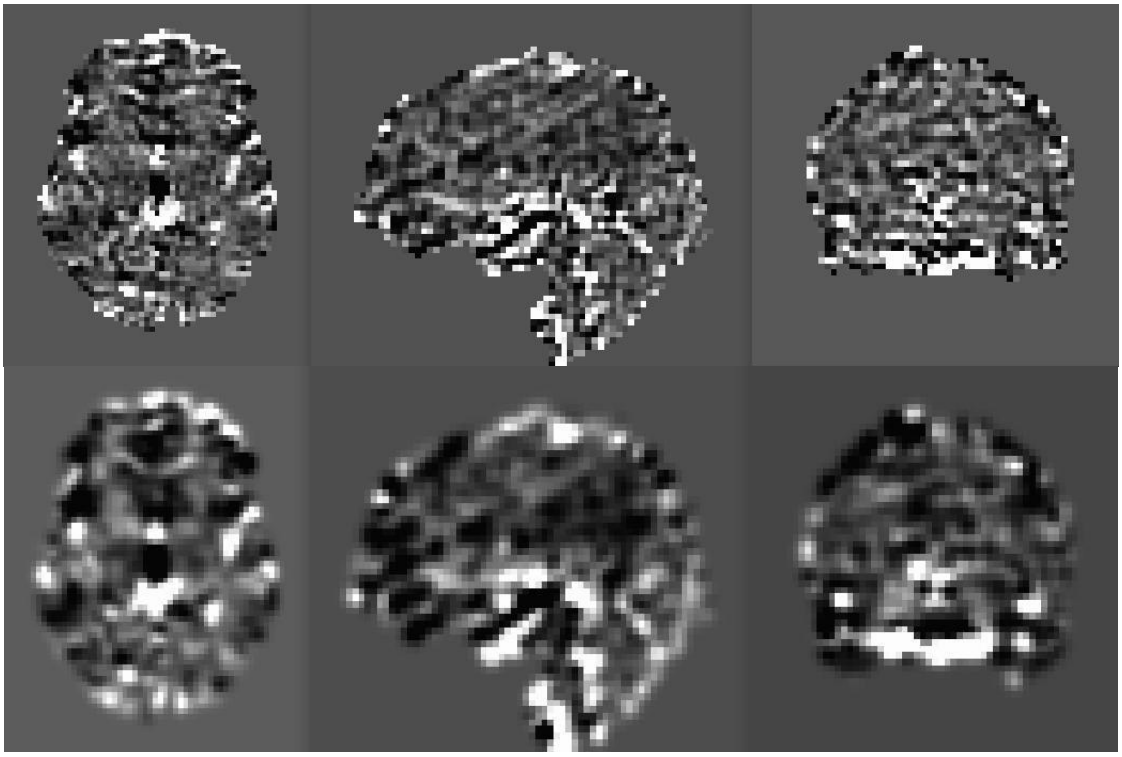

Figure 3.8 Differences between outputs after filtration (top) and smoothing (bottom) of a single scan from the study.

CHAPTER 4

FUNCTIONAL CONNECTIVITY AND STATISTICAL ANALYSIS

Functional connectivity is the temporal correlation of 2 or more neurophysiological signals at spatially different locations in the brain. These events can be analyzed either in the time or frequency domain. Temporal analysis can provide information about the changes within a given time series in an fMRI dataset. Frequency analysis can provide information about the frequency content of the events that are happening in a particular fMRI dataset. These techniques can also be designated into either a model-driven or a data-driven analysis. Each model can include either frequency analysis or temporal analysis methods. Model-driven methods are useful when there is some prior information about the current dataset and research topic, while data-based methods make no such assumptions and finds the areas of interest according to the fMRI data provided. In this study, data-driven methods are mostly used, and the only model-driven approach would be the three regions that were identified from the Independent Component Analysis (ICA) (Azeez & Biswal, 2017, Buckner et al., 2013, Chen et al., 2020, Friston, 1994).

Table 4.1 Methods Used For This Study

Methods	**Data-Driven**
Temporal	ICA, ReHo
Frequency	ALFF, mALFF, fALFF

After the completion of the various analyses, the results were inputted into a multiple linear regression model to find their significance in terms of P-values, as explained in section 4.3. Furthermore, the effects of age and gender were evaluated and explained in Section 4.4.

4.1 Temporal Domain Methods

4.1.1 Independent Component Analysis (ICA)

ICA is a popular data-driven method in neuroimaging. ICA is a method like PCA with a crucial difference: while the PCA method estimates components that are orthogonal, ICA generates components that are independent of each other. PCA cannot accomplish this because it assumes a Gaussian distribution (Azeez, 2019, Azeez & Biswal, 2017, Hafiz, 2017). With ICA, we obtain independent components for the fMRI images. This means that for the rs-fMRI data, we can see the resting state networks from the analysis. From the spatial maps, there is a challenge in linking these spatial maps to neurological function. It is also a way of confirming the quality of the data and preprocessing. Generally, after ICA for rs-fMRI data, there is a certain number of resting state networks that a researcher expects to see (Azeez & Biswal, 2017, Calhoun et al., 2003, Chen et al., 2008, Smitha et al., 2017).

For this study, a group ICA was applied to the dataset after the pre-processing procedure. Group ICA was performed using the MELODIC feature from FSL (the FMRIB Software Library) (Jenkinson et al., 2012). Three sessions were made using 20, 25, and 30 component ICA. The reason for these choices was to achieve the best ICA components while avoiding a mixture of components to form (Beckmann et al., 2005). In the 20 component ICA, some resting state networks that needed to be separate were mixed into a single spatial map. With the 30 component ICA, some resting state networks that needed to be a single spatial map were separated into multiple maps. The best results were acquired using a 25 components ICA. From the 25 component ICA analysis, 3 probability maps were used to create masks with the SPM12 image calculator to be used in further steps of the analysis. For the masks, a threshold value of 0.95 was used.

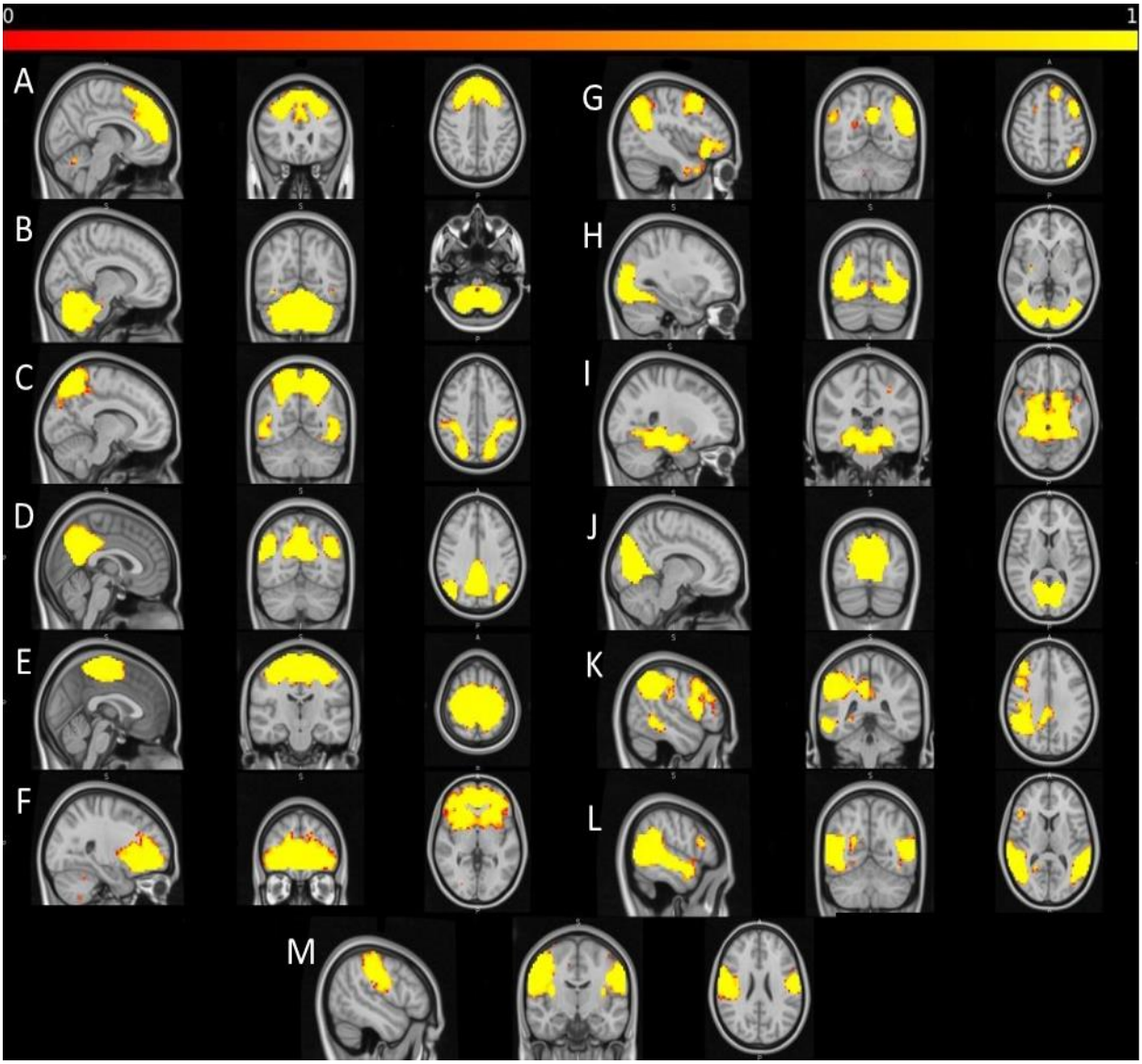

Figure 4.1 Resting state networks generated from group independent component analysis. A. aDMN (anterior default mode network), B. CN (cerebellar network), C. DA (dorsal attention), D. DMN (default mode network), E. dSM (dorsal sensory motor), F. FC (frontal cortical), G. LFP (left frontoparietal), H. LV (lateral visual), I. MT (medial temporal), J. MV (medial visual), K. RFP (right frontoparietal), L. VS (ventral stream), M. vSM (ventral sensory motor) (sagittal – coronal – axial view).

4.1.2 Regional Homogeneity (ReHo)

Regional Homogeneity, also known as ReHo, is another data-driven approach. This method applies a voxel by voxel approach to map underlying connectivity activations within the brain. As the name suggests, ReHo finds the average correlation with its neighboring voxels for every voxel in the brain. To check for the correlation between voxels, Kendall's correlation

coefficient (KKC) is used in conjunction with the size of the clusters (Zang et al., 2004). ReHo is considered to be a robust method against noise but is still susceptible to signal artifacts and can cause false positive results. Local functional connectivity is the synchronized response of a BOLD time series for the functional activations in a given 10-15 mm region. Based on the hypothesis of significant brain function, these 27 voxels or 10-15 mm area are active in a form of cluster rather than a single voxel. (Azeez & Biswal, 2017, Bayram et al., 2018, He et al., 2007, Jiang & Zuo, 2016, Liu et al., 2008).

In this study, the masks created from the probability maps acquired from group ICA analysis are used on the ReHo maps. The ReHo spatial maps are generated using AFNI. Outputs of temporal regression and filtration were used to generate ReHo spatial maps. Using the masks on the spatial maps, the mean value for each fMRI scan were calculated using MATLAB to be used later in multiple linear regression analysis (Di et al., 2019). Lastly, outputs of ReHo were smoothed using SPM12.

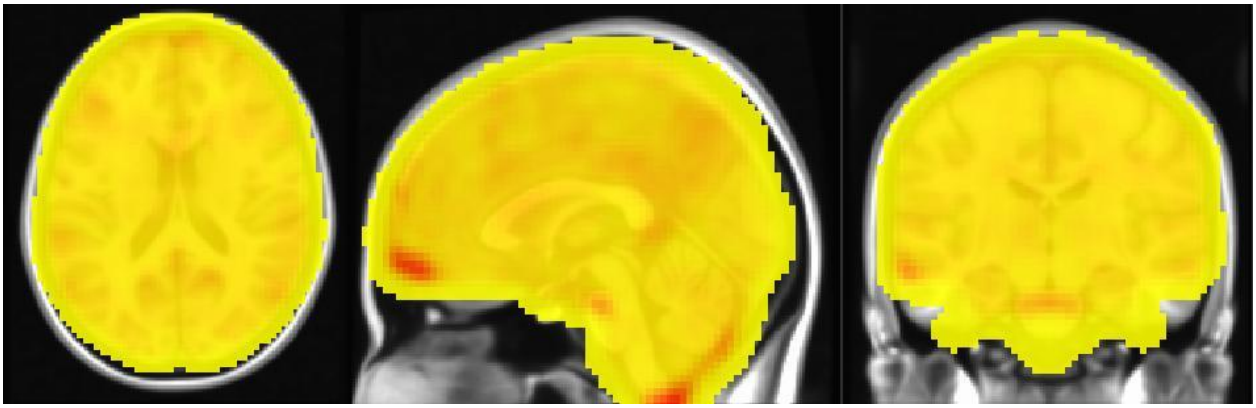

Figure 4.2 Regional homogeneity of an anonymous subject from the current study overlaid on MNI template (axial – sagittal – coronal view).

4.2 Frequency Domain Methods

4.2.1 Amplitude of Low Frequency Fluctuations (ALFF)

In rs-fMRI, functional connectivity is highly correlated with low frequency fluctuations. ALFF presumes that all neurological activity in a BOLD signal from rs-fMRI can be shown with a singular parameter. In short, it takes the square root of the power of BOLD signals in 0.01-0.1 Hz range and sums it up to obtain the ALFF value. This method is sensitive to noise sources; hence, quality and preprocessing of the raw data plays an important role in ALFF. Because ALFF might have noisy signals, there will be a higher probability of a large ALFF value. An alternative method called fractional ALFF (fALFF) can also be used. In fALFF, the ALFF value is divided by the spectral power for the entire power spectrum. This method also may produce low quality spatial maps caused by low quality in fMRI scans, but it may produce significant results when provided with quality rs-fMRI scans (Zou et al., 2008). Another version is the global mean ALFF (mALFF). In mALFF, as the name suggests, each voxel in ALFF gets divided by the global mean of ALFF (Yang et al., 2019, Fox & Raichle, 2007).

The masks created from the probability maps acquired from group ICA analysis are used on the ALFF, fALFF, and mALFF maps (figure 4.4). These spatial maps are generated using AFNI. Outputs of temporal regression were used to generate ReHo spatial maps. Using the masks on the spatial maps, the mean value of each fMRI scan and each spatial map were calculated using MATLAB to be later used in the multiple linear regression analysis (Di et al., 2019). Lastly, all ALFF, fALFF, and mALFF outputs were smoothed using SPM12.

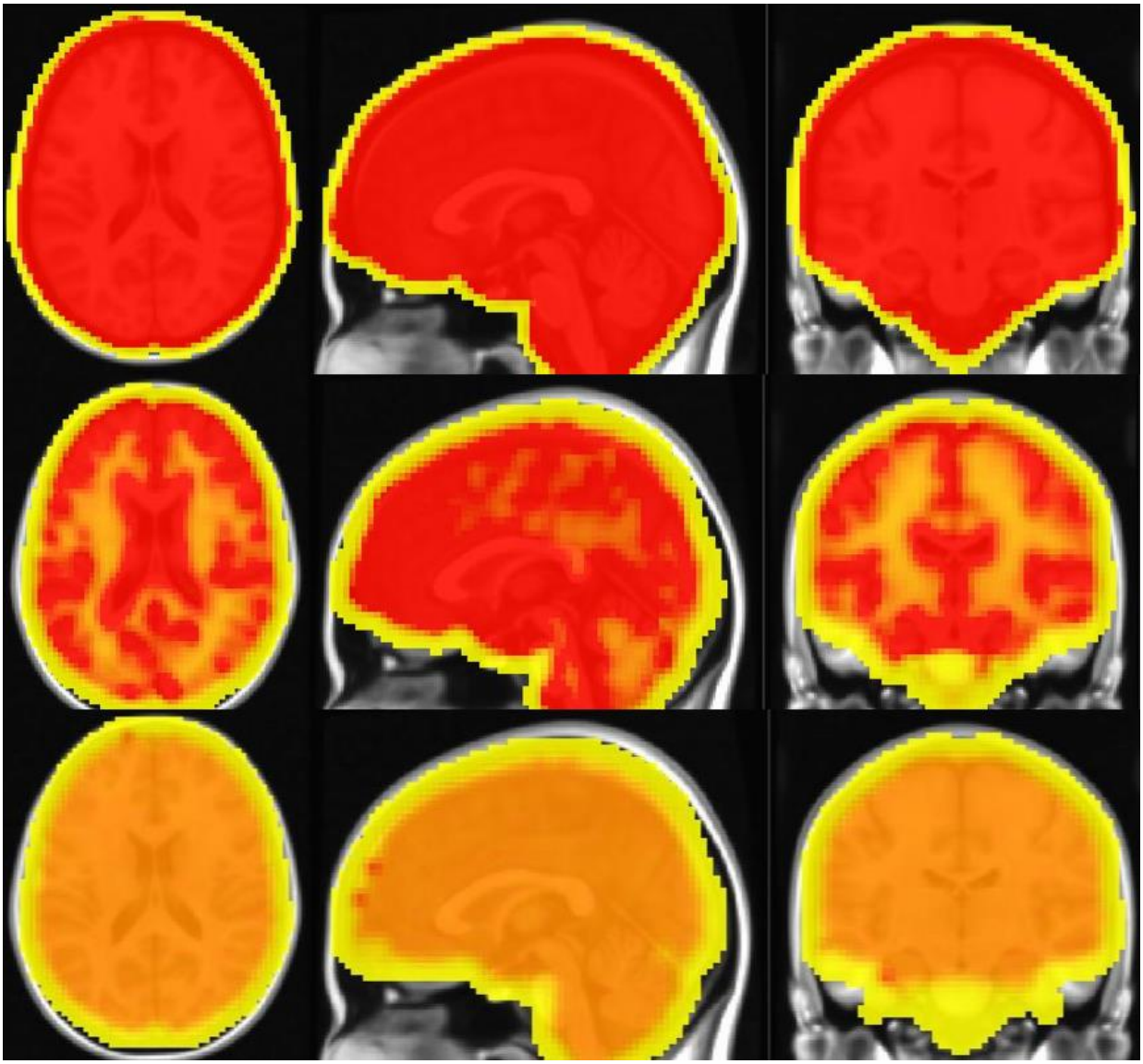

Figure 4.3 ALFF (top), mALFF (middle), fALFF (bottom) of an anonymous subject from the current study overlaid on MNI template (Axial – Sagittal – Coronal view).

4.3 Multiple Linear Regression Analysis

In this study, all the spatial maps from ALFF, mALFF, fALFF, and ReHo are used with 3 masks generated from the probability maps from ICA to get individual mean values for specific regions. The regions used are the Default Mode Network (DMN), the Medial Visual Network (MV), and the Medial Temporal Network (MT). A value, or score, is generated for each spatial map and used within the multiple linear regression analysis. Other than the ALFF, fALFF, mALFF, and ReHo score, the age of the subjects and category (AD or HC) of the subjects are

also used in the equation. R Commander was used to do these calculations (Fox & Bouchet-Valat, 2020).

$$Y = \beta_0 + \beta_1 X_1 + \beta_2 X_2 + \beta_3 X_1 X_2$$

Figure 4.4 Formula used for multiple linear regression analysis.

As can be seen from the formula (figure 4.5), both predictors X1 and X2 create a third predictor by multiplication. In other words, the third coefficient is influenced by the first two predictors. Even if the P value of one of the first two predictors is not significant, it may still be significant for the third feature. Similarly, if the first two features are significant, there is no guarantee that the third feature will be significant. This is called the hierarchical principle, and it basically means that two non-significant individual models could have significance when they interact. For this study, our predictors are age of the patients and the group they are in (HC or AD).

4.4 Statistical Analysis of the Participants

In the study, some subjects were removed due to several reasons. These reasons were: high motion that cannot be corrected, corrupted/missing rs-fMRI or anatomical images, and incompatible number of time points. Following the removal, the Shapiro-Wilk and Shapiro-Francia Normality Test, the Levene's Homogeneity Test, and a two-sample t-test had been performed for age. For gender, the Chi-squared test had been performed. In the study, there are 61 individuals (33 are female and 28 are male). The age range of the participants is 56 to 91. The mean of these ages is 74.4721 and standard deviation is 7.0408 (figure 4.6).

The P value of the Shapiro-Wilk and Shapiro-Francia Normality Test was 0.6663, which indicates that normality was met. The P value of the Levene's Homogeneity Test was 0.6836,

which means homogeneity was met. The P value of the Two Sample T-Test was 0.1129, which means age should not affect the analysis. Similarly, the P value of the Chi-Square test was 0.9061, which means gender should not affect the analysis.

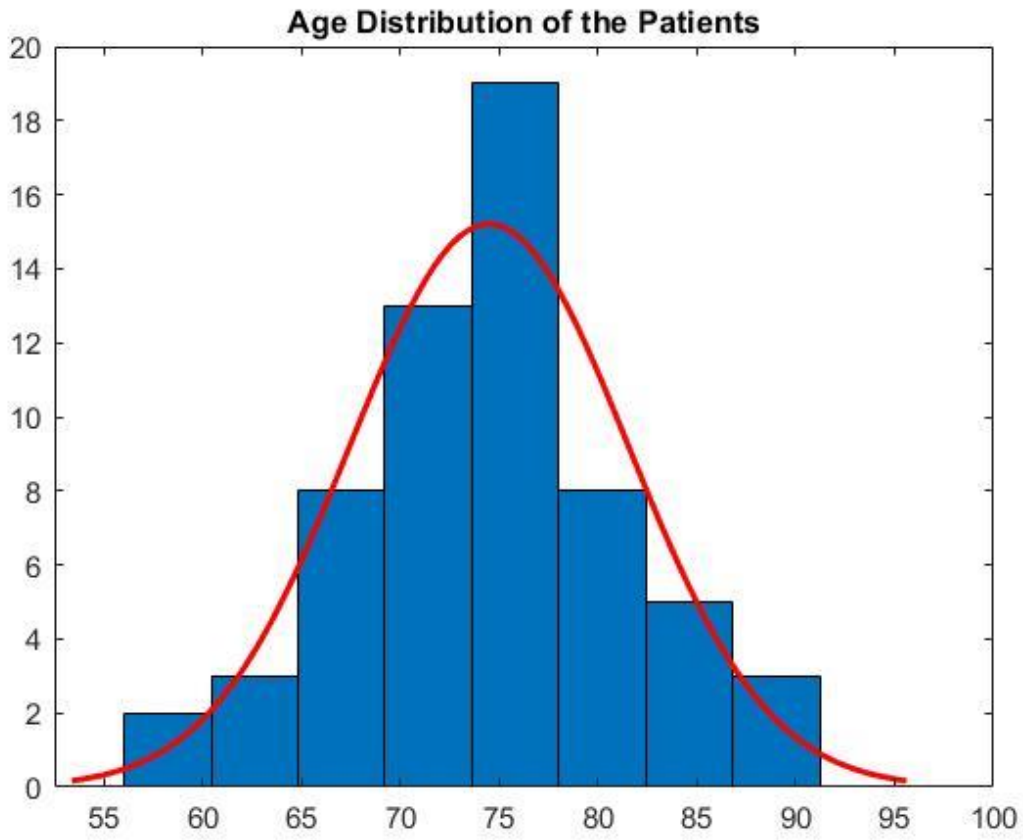

Figure 4.5 Age distribution of the participants (x – axis: age, y – axis: quantity).

CHAPTER 5

RESULTS

This chapter will focus on the results obtained in this study. After preprocessing, there were 76 scans for AD and 79 scans for HC, adding up to a total number of 155 scans used within the study. Voxel-wise functional connectivity parameters were obtained using several methods, including ICA, ReHo, ALFF, mALFF, and fALFF. Spatial component maps were generated using ICA. Voxel wise parameters from each of the spatial maps were obtained using ReHo, ALFF, mALFF, and fALFF. Twelve different scores were generated from the dataset using the twelve plots made from the score, age, and category of the subjects. From the 12-score set, 6 of them (mALFF and ReHo) matched the results of previous studies, and the other 6 (ALFF and fALFF) were in low quality caused by low-quality scans (high head motion). Thus, spatial maps from ALFF and fALFF were not able to be used for further analysis. The six score sets that were acceptable were used to do a multiple linear regression analysis. For the analysis, every scan was presumed to be from a different subject even if several scans were taken from the same patient.

5.1 Region of Interests

After preprocessing, a group ICA was performed using data from all 155 individual scans. A total of 13 meaningful resting-state networks were determined from ICA, as shown in figure 4.1 (Calhoun et al., 2003, Beckmann et al., 2005). From the probability maps generated with ICA, three maps were chosen to use as ROIs (figure 5.1). These ROIs were created by thresholding the probability maps. Selection of ROIs was done according to previously published literature.

In previous studies, it has been showed that the MT is one of the regions that gets affected from AD. Furthermore, it has been shown in functional brain imaging that these abnormalities occur before atrophy starts to present itself in the early stages of AD (Grajski & Bressler, 2019, Qi et al., 2018). The hippocampus in the MT is involved with memory, and memory loss is one of the major symptoms that AD patients suffer from. Subsystems which deal with memory are also linked to the DMN, which suggests that the FC of DMN also gets affected (Qi et al., 2018). Because of this dilemma, it is expected to see decreased FC in the MT caused by the WM atrophy in AD patients (Berron et al., 2020), which is an easy symptom to miss in early stages of the disease with only a physical examination. The MT shows potential to be used as a neuroimaging biomarker for early detection of AD, which is also supported by metabolic abnormalities that can be seen within the network (Mevel et al., 2011, Greicius et al., 2004, Ridha et al., 2007).

The DMN is a network that is connected to various regions within the brain and is one of the regions that has high potential to be used as a neuroimaging biomarker for early detection of AD (Badhwar et al., 2017). FC changes in the DMN are highly corelated with AD, especially in the precuneus (PCC) (Mevel et al., 2011). Connectivity between the PCC and hippocampus suggests that the DMN could also be a potential neuroimaging marker for early AD detection (Mevel et al., 2011). Although the DMN is a region that is highly used to separate HCs from AD patients, the diagnostic power of the DMN as a neuroimaging biomarker is yet to be seen because of high baseline FC of certain regions within the DMN (Koch et al., 2012). Past studies also show that though there were no statistical difference between HCs and mild cognitive impairment (MCI) patients, there were similarities at the PCC of the DMN (Wu et al., 2011, Yu et al., 2016). Furthermore, past studies show that MMSE values of AD patients seem to be linked with FC decreases within the DMN in AD patients, possibly strengthening the diagnostic

power of DMN as a neuroimaging biomarker (Buckner et al., 2008, Sorg et al., 2007, Wu et al., 2011).

Visual performance also decreases with AD, which suggests that the primary visual cortex could show FC differences in patients with the disorder (Armstrong,1996, Mendez et al., 1990, Leuba & Kraftsik, 1994, Yamasaki et al., 2019). Nevertheless, there are some controversies about this, since only some clinical studies show visual performance differences between AD and MCI patients when compared with HCs (Armstrong, 2009). It is also important to consider any other conditions that may impact the patient's eyesight before using visual performance as a parameter to differentiate HCs from AD and MCI patients. Since it is difficult to determine the primary reason for an impaired visual performance, FC differences between HCs and AD patients in the primary visual or the MV network can be a potential neuroimaging biomarker. Previous studies showed markers linked to AD were found not only within the primary visual cortex, but also on certain components of the eyes itself (Armstrong, 1996, Beach & McGeer, 1992, Ikonomovic et al., 2005, Kusne et al., 2017). While clinical tests show abnormalities in terms of visual function in both AD and MCI patients, there are not many rs-fMRI and FC studies performed about this region (Cerquera-Jaramillo et al., 2018, Kusne et al., 2017). Overall, the MV network shows potential to be a neuroimaging biomarker for AD, and is also one of the ROIs that has been investigated within this study (Bokde et al., 2006).

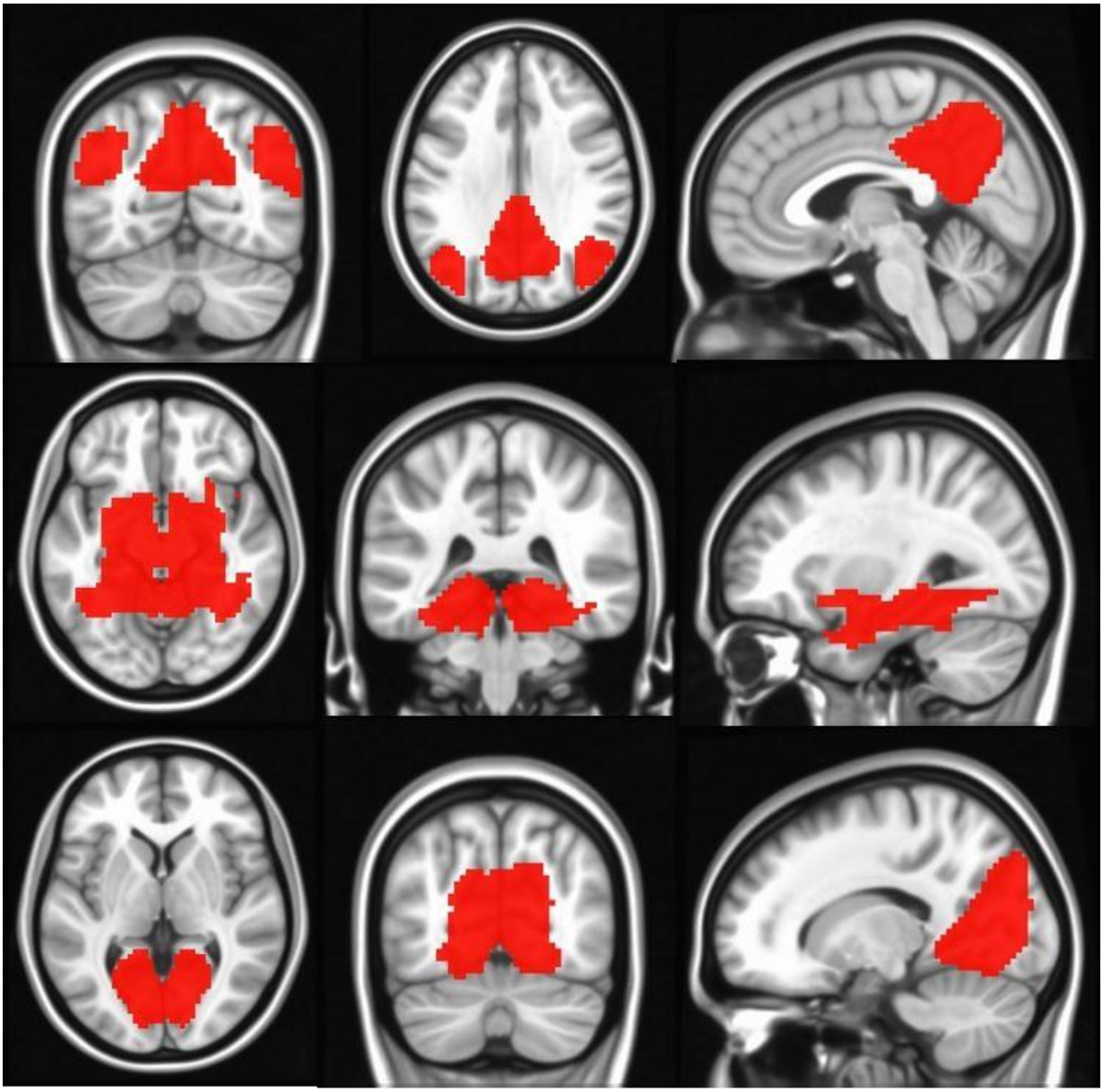

Figure 5.1 ROIs created from probability maps acquired from ICA. DMN (top), MT (middle), MV (bottom) (axial – coronal – sagittal).

5.2 Local Activity

As mentioned earlier, three ROIs were used: DMN, MV, and MT. For each of the three resting state networks, we also generated mALFF and ReHo scores on a voxel-wise basis. By doing this, six scores were generated for each scan. These scores were: DMN-mALFF, DMN-ReHo, MT-mALFF, MT-ReHo, MV-mALFF, MV-ReHo. By using these scores as the y-axis and the current age of the subject as the x-axis for every 155 scans, their plots were generated according

to their groups (AD or HC). For each graph and each data point in the graphs, linear regression was used to determine the relationship between the two parameters in the graph. Scores were plotted as a function of age (Di et al., 2019).

5.2.1 Local Activity Differences for DMN

Figure 5.2 and Figure 5.3 show local activity differences in the DMN region from the mALFF and ReHo measures. In various studies, it has been shown that the DMN region has a role in AD (Mevel et al., 2011, Koch et al., 2012). The DMN has a major role in rs-fMRI studies and is a widely studied brain network in the neuroimaging world. The DMN is known to have high-level metabolic activity during the passive state. This means that for rs-fMRI scans, the DMN should have high local and metabolic activity. Also, previous neuroimaging studies made with spontaneous low-frequency fluctuations and regional homogeneity show that it is linked to crucial subsystems (Sheline et al., 2010). It links various regions such as the precuneus cingulate cortex to these subsystems (Wang et al., 2006). Various studies show that impairment of DMN is a result of AD (Bayram et al., 2018, Marchitelli et al., 2018, Qi et al., 2018).

As can be seen from Figure 5.2 and Figure 5.3, AD patients show decreased local activity for mALFF and ReHo measures within the DMN region for the dataset used in this study. From Figure 5.2 and Figure 5.3, we can also see that age has a decreasing effect in the DMN-mALFF and DMN-ReHo scores. By using the formula from Figure 4.4, a hierarchical model was used to perform a multiple linear regression analysis to see the effect of age and condition on the DMN-mALFF and DMN-ReHo scores. The purpose of this longitudinal analysis is to determine if the decrease in local activity or functional connectivity is different between HC and AD, and can be explained using age, condition, or both.

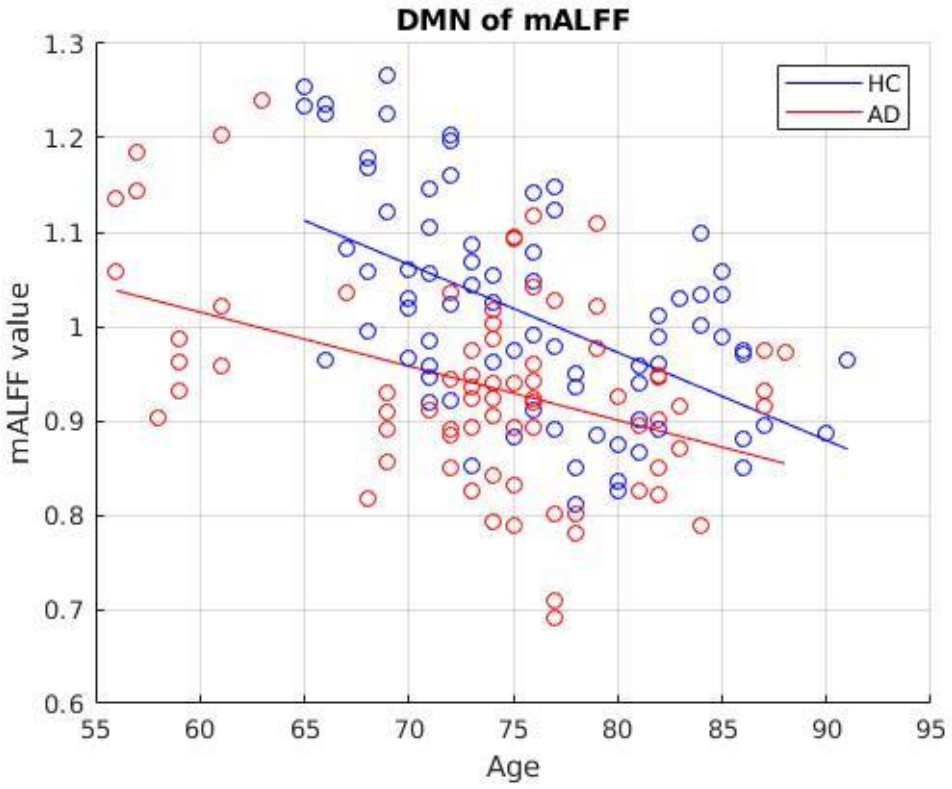

Figure 5.2 DMN-mALFF graph.

Table 5.1 P Values From DMN Of mALFF Graph

P-value of AGE feature	0.000000328
P-value of GROUP feature	0.0377*
P-value of AGExGROUP feature	0.1168

Figure 5.2 illustrates a negative relationship between the dependent variable (mALFF) and the independent variable (age). The attained P values display a decrease in the dependent variable and an increase in the independent variable. Therefore, the P-value highlights that age is not a significant determiner, and that this focus hypothesis was not met (Table 5.1).

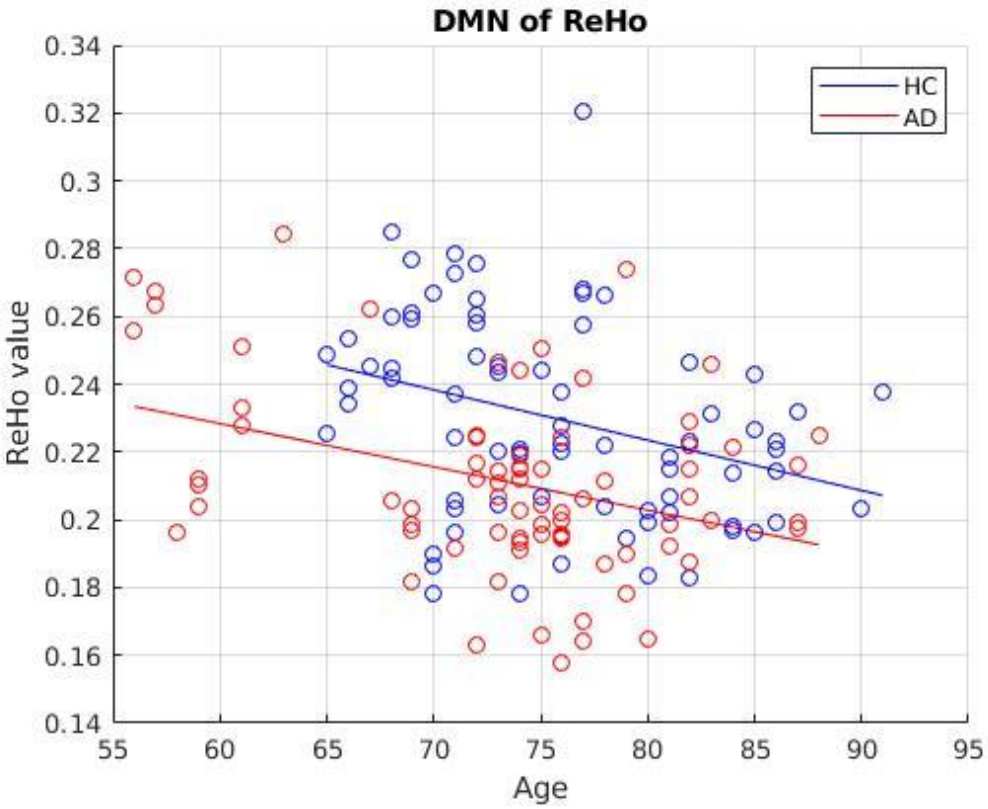

Figure 5.3 DMN-ReHo graph.

Table 5.2 P Values From DMN Of ReHo Graph

P-value of AGE feature	0.00182*
P-value of GROUP feature	0.41757
P-value of AGExGROUP feature	0.73272

In comparison, Figure 5.3 justifies that the DMN-ReHo graph displays a negative relationship between the variables. However, the results attained were not significant, as the P-values did not exceed 0.05 for the last two features (Table 5.2). As highlighted before, the DMN includes the following regions within its boundaries: the posterior cingulate cortex (PCC) or precuneus, the ventral and dorsal medial prefrontal, the medial temporal lobes, and the lateral parietal cortices. Furthermore, the posterior cingulate cortex and the hippocampus is impaired in AD in terms of FC. Other scholarly deductions state that PCC atrophy is a result of long-term effects

of brain disconnections that further worsen the progression of AD on the patient. Furthermore, when age is factored in as a variable utilizing the two-sample T-test, a 0.1129 P-value affirmed that age would not affect the linear regression analysis results.

5.2.2 Local Activity Differences for MT Lobe

Figure 5.4 and Figure 5.5 show local activity differences in the MT region from mALFF and ReHo measures. Previous studies showed that the MT is affected in the brains of AD patients. The MT lobe includes the hippocampus and has a vital role in terms of memory. The MT is responsible for several cognitive and emotional functions. Atrophy of the MT lobe is a common finding in many studies (Ridha et al., 2007). Furthermore, many PET studies also show that metabolic activity also differs between HCs and AD patients for the MT lobe (Fischer et al., 2019, Mevel et al., 2011, Márquez & Yassa, 2019). This suggests that regional brain atrophy of the MT lobe has a role in the corresponding resting state activity, and AD patients present symptoms like verbal memory decline, episodic memory decline, visual memory decline, memory recall delay increase etc. (Mevel et al., 2011, Gilboa et al., 2015, Yamashita et al., 2019). Also mentioned above, the MT lobe is a subsystem of DMN, which means a local activation decrease at DMN would also show itself in a local activity decrease at the MT lobe. In other words, sub-regions of the MT lobe that deals with memory are major locations that get affected in AD patients. Since MT is a subsystem of DMN, it is logical to presume memory decline and decreased local resting activity in DMN means a decreased local activity for the MT lobe (Bayram et al., 2018, Berron et al., 2020, Liu et al., 2008, Rombouts et al., 2005).

As can be seen from Figure 5.4 and Figure 5.5, AD patients show decreased local activity for mALFF and ReHo measures within the MT lobe region for the dataset used in this study. However, from Figure 5.4 and Figure 5.5, we can also see that age has a decreasing effect in MT-mALFF and MT-ReHo scores, just like in the DMN-mALFF and DMN-ReHo scores.

Using the formula from Figure 4.4, a hierarchical model is used to do a multiple linear regression analysis to see the effects of age and condition on the MT-mALFF and MT-ReHo scores.

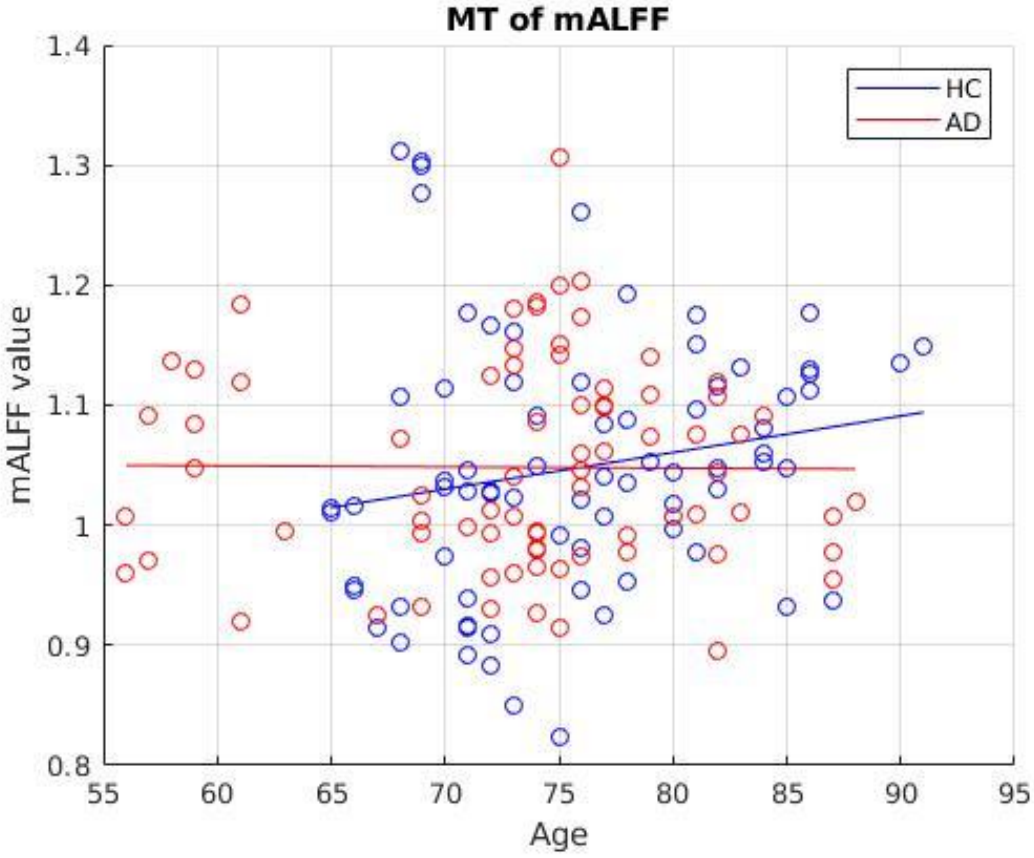

Figure 5.4 MT-mALFF graph.

Table 5.3 P Values From MT Of mALFF Graph

P-value of AGE feature	0.0733
P-value of GROUP feature	0.1530
P-value of AGExGROUP feature	0.1566

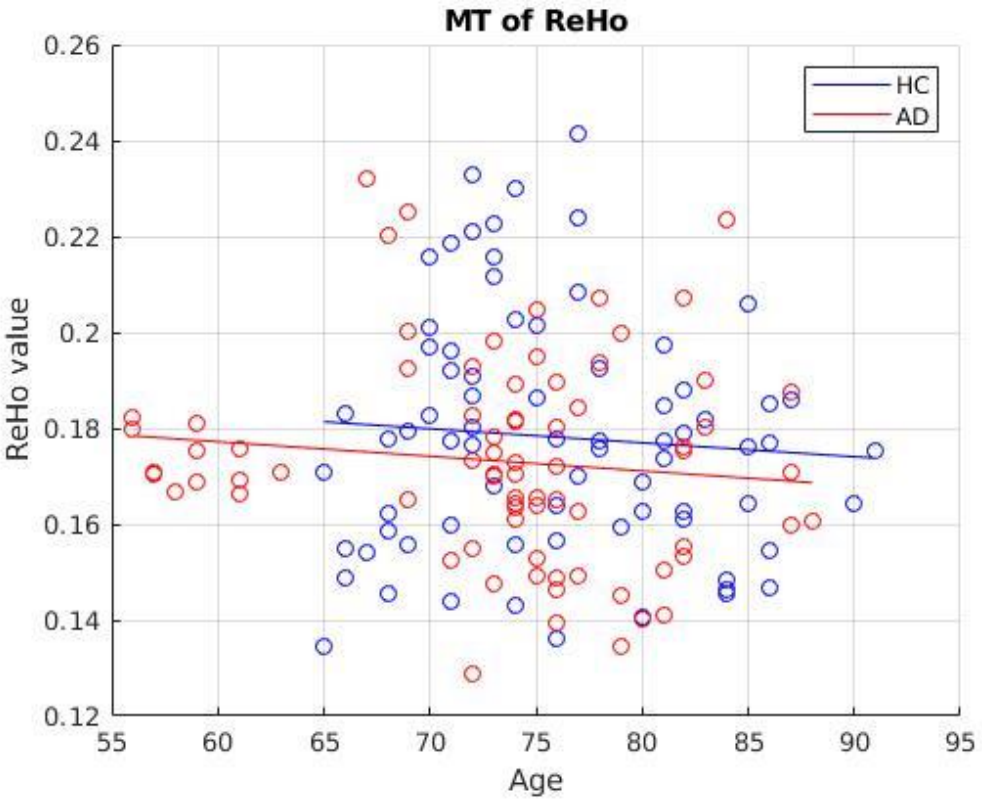

Figure 5.5 MT-ReHo graph.

Table 5.4 P Values From MT Of ReHo Graph

P-value of AGE feature	0.473
P-value of GROUP feature	0.903
P-value of AGExGROUP feature	0.1566

Figure 5.4 illustrates the relationships between the MT and mALFF, where the dependent variable was the mALFF of MT while the independent variable was age. In contrast, for the AD results, the line projects a negative relationship in which when the y-variable increases, the age variable correlates towards the reduction plane for AD. The P values prove significant in the context of AD and HC groups, respectively. Studies support that frontotemporal dementia in young people is the precipitating factor, which is common in people under 65 years (Rossor et

al., 2010, Rombouts et al., 2005, Smitha et al., 2017, Yetkin et al., 2006). In Figure 5.4 and Figure 5.5, the P-value hardly meets a 0.05 threshold to be significant (Table 5.3 & Table 5.4).

To check for the correlation between the voxels, Kendall's correlation coefficient (KKC) is used. The size of the clusters that are found is around 27 voxels. The method is used to describe local functional connectivity at a given voxel and its neighboring voxels. Local functional connectivity refers to the synchronized response of the BOLD time series for functional activations in each 10-15 mm region. Based on the hypothesis of significant brain function, these 27 voxels, or 10-15 mm area, happen in the form of a cluster rather than a single voxel. Figure 5.4 and 5.5 illustrate that in the MT during early AD, FC of the hippocampus decreases according to HCs.

5.2.3 Local Activity Differences for Primary Visual Network

Figure 5.6 and Figure 5.7 show local activity differences in the MV region from the mALFF and ReHo measures. Unlike the DMN or MT lobe, the visual cortex has not been as widely studied in AD patients within the neuroimaging world. It is known that AD also affects the visual system. Although AD is mostly known to affect cognitive function, there are also known effects on various sensory functions, such as the visual systems. Visual dysfunctions in AD are possible neuroimaging biomarkers at the functional level. Nevertheless, there are fairly few neuroimaging studies done on the visual cortex in AD. AD is known to cause reduced retinal thickness, retinal vasculature, and quantity of optic nerve axons. Furthermore, visual problems show themselves in early AD. Some of these are visual acuity, contrast sensitivity, color discrimination, visual-special perception, the processing speed of visual information, and visual-spatial attention. Because of all these dysfunctions, it is possible and logical that AD patients would show decreased local activity in the Medial Visual (MV) network in rs-fMRI

(Armstrong, 2009, Cerquera-Jaramillo et al., 2018, Kusne et al., 2017, Leuba & Kraftsik, 1994, Zhang et al., 2009).

As can be seen from Figures 5.6 and 5.7, AD patients show decreased local activity for mALFF and ReHo measures within the MV lobe region for the dataset used in this study. From Figure 5.6 and Figure 5.7, we can also see that age has a decreasing effect in MV-mALFF and MV-ReHo scores, just like in the DMN-mALFF, DMN-ReHo, MT-mALFF, and MT-ReHo scores. Using the formula from Figure 4.4, a Hierarchical model is used to do a multiple linear regression analysis to see the effect of age and condition on the MV-mALFF and MV-ReHo scores.

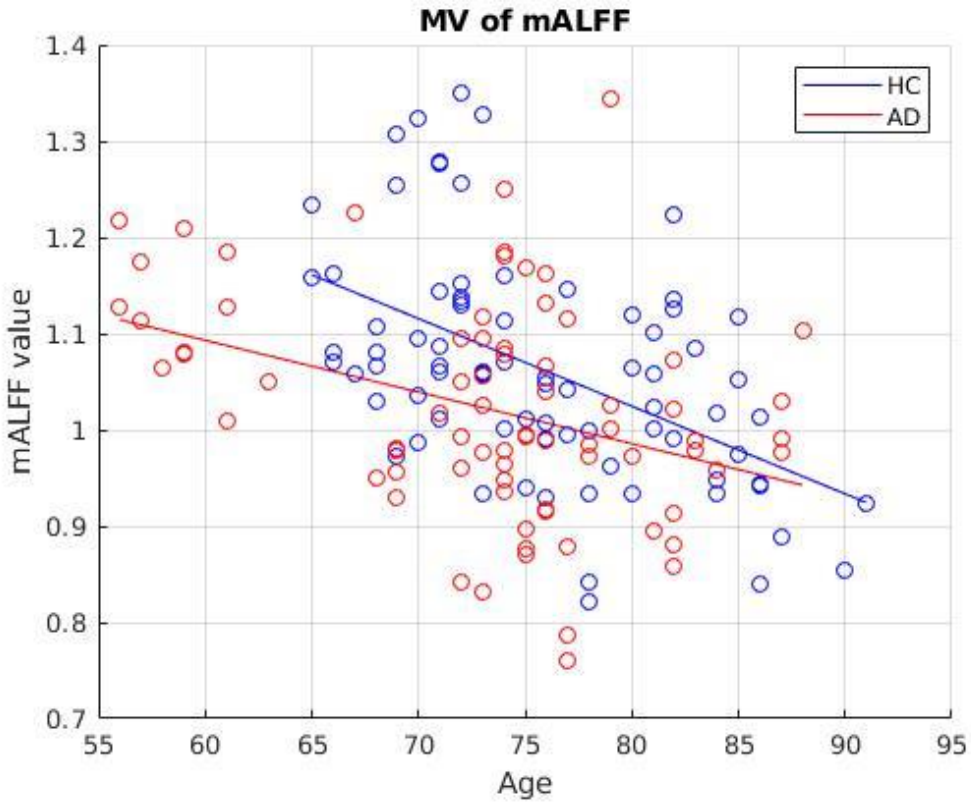

Figure 5.6 MV-mALFF graph.

Table 5.5 P Values From MV Of mALFF Graph

P-value of AGE feature	0.00000162 *
P-value of GROUP feature	0.0615
P-value of AGExGROUP feature	0.1191

To investigate brain activity in people with impaired cognitive activity, changes concerning the brain structure as well as function are of vital concern. Figure 5.6 did not meet a 0.05 threshold for the last two features (Table 5.5). This implies that the (P<0.0615) value is insignificant.

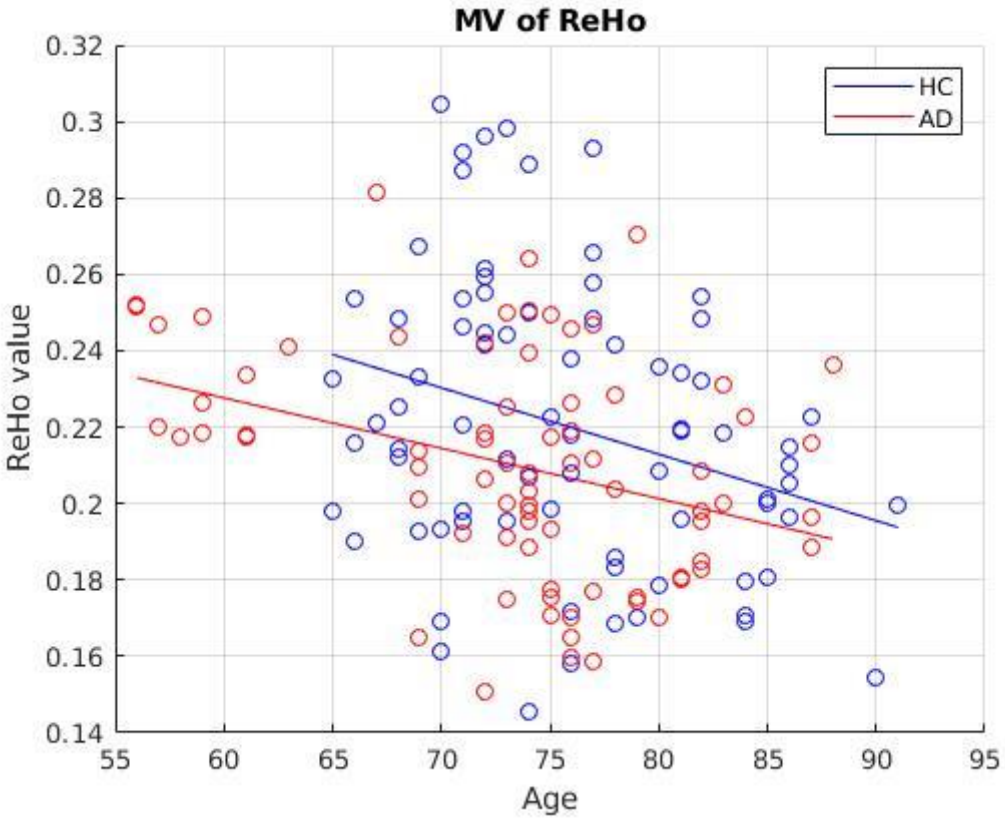

Figure 5.7 MV-ReHo graph.

Table 5.6 P Values From MV Of ReHo Graph

P-value of AGE feature	0.00241*
P-value of GROUP feature	0.41471
P-value of AGExGROUP feature	0.56839

ReHo or mALFF of BOLD signals, as delineated in Figure 5.6 and Figure 5.7, have assessed changes in the resting state occipital cortex of this study's respondents. Both effects could exist together in either MCI of AD. The diminished FC in the cuneus/precuneus was considered to be related to decreased memory execution, and the expanded action could be paying for harm by the enlistment of different regions such as MV. It is also a known that AD affects atrophy in WM, which includes visual mechanisms that can cause FC changes in GM at MV. Nevertheless, the analysis only showed the AGE feature to be statistically relevant.

CHAPTER 6

DISCUSSION AND CONCLUSION

The current study investigated rs-fMRI scans of AD patients and healthy controls to identify differences between the two groups. Spatial maps, generated from the rs-fMRI scans of the AD patients and the HCs and analyzed using several multiple linear regressions, were used to compare the two groups in a longitudinal approach. The discussion section further examines the outcomes of this functional connectivity analysis.

6.1 Discussion

This study, although unable to show statistically significant results with the AGExGROUP feature of the equation, does show expected local activity differences between HCs and AD patients as a function of age in the patterns within the graphs. The purpose of this study was to measure local activity differences with a ROI-based hypothesis using the Hierarchical Principle with rs-fMRI scans. In further studies with a similar approach, and with a more controlled (stages of the disease) and more quality dataset, it is possible to generate statistically significant results. The importance of this approach is to be able to identify biomarkers for AD to be used in popular methods such as machine learning and graph theory (Huf et al., 2014, Khazaee et al., 2015). In other words, finding potential neuroimaging biomarkers from a detailed and high-quantity rs-fMRI AD dataset has potential to be used as diagnostic tools on future patients to start their treatment as soon as possible. This would help with the diagnosis of the disease, since it is expected that the number of AD patients will drastically rise in the future. In AD, early detection and diagnosis of the disorder are generally not easy to make, and late treatment loses its effectiveness. Furthermore, early symptoms are easy to mix with those of becoming elderly. This means that symptoms of aging and symptoms of early AD are similar to each other.

6.1.1 Functional Connectivity (FC)

To begin, the standard longitudinal analysis failed to produce any significant outcomes in this study. In the current study, the graph displays significance in the DMN and the MV, which impacts the age variable inversely instead. In contrast, the inter-network functional activity evolves with age, and the anti-correlated activity between the dorsal attention network and the DMN also significantly minimizes with age. Past research indicated that reduced FC raised the hypothesis that cortical hubs, including PCC, are susceptible to functional deterioration as a result of their relatively high metabolism (Qi et al., 2018), which is no longer maintained due to amyloid deposition that co-occurs in these hubs (Berron et al., 2020). Despite the consistency with the literature of the observed FC outcomes pointing out lower connectivity in AD, the research findings did not indicate reductions in the DMN network that were statistically significant on a robust level. Some of the main reasons for this could be because: a limited number of scans since data-driven methods function better with more data; a limited amount of information about the scans could suggest the possibility that the progression of the disease might be quite different for each patient; and the quality of the dataset that might have caused false negative results.

6.1.2 Impairment of DMN is a Result of AD

The results of the mALFF of the DMN indicated that AD patients show decreased local activity for mALFF as well as ReHo measures within the DMN region for the dataset included in this study. The relationship between localized neural activity and dynamic connectivity in the two core regions of the DMN was identified through directionally asymmetric and particularly specific ROIs: DMN, MV, and MT. AD patients showed decreased local activity for mALFF and ReHo measures within the MV region for the dataset applied for the current research study.

However, further analysis indicates that age has a considerable impact, since it has a reducing impact in MV-mALFF ($P_{age\text{-}MV\text{-}mALFF}$ =0.00000162) and MV-ReHo ($P_{age\text{-}\ MV\text{-}ReHo}$ = 0.00241) scores similar to the DMN-mALFF ($P_{age\text{-}DMN\text{-}mALFF}$ = 0.000000328**)**, DMN-ReHo ($P_{age\text{-}DMN\text{-}ReHo}$ = 0.00182), MT-mALFF ($P_{age\text{-}MT\text{-}mALFF}$ = 0.0733), and MT-ReHo ($P_{age\text{-}MT\text{-}ReHo}$ = 0.473) scores. As can be seen from the P values in the multiple linear regression analysis of the graphs (Chapter 5), 4 out of 6 measures were significant for the age feature. Furthermore, group features of the DMN-mALFF also showed significance with a multiple linear regression analysis ($P_{group\text{-}DMN\text{-}mALFF}$ = 0.00377**).** When investigating rs-fMRI scans of individuals with impaired brain cognitive activity from the study, a multiple linear regression analysis with the mALFF and ReHo of 3 ROIs did not show significance for the third feature of the equation (AGExGROUP). Hence, the p values (P>0.5) are statistically insignificant. Therefore, this study shows that the hypothesis was not achieved.

6.1.3 DMN in AD Patients

From the study, DMN activity among AD patients is consistent with those found using the PET measure of resting-state brain metabolism and this shows the significant involvement of the PCC region for examinations through rs-fMRI scans for AD (Mevel et al., 2011, Marchitelli et al., 2018). Increments in DMN connectivity or activity have likewise been accounted for in patients with MCI when contrasted with AD (Gardini et al., 2015, Zhang et al., 2012). Along these lines, amnestic mild cognitive impairment (aMCI) patients were described by (i) increments in DMN activity situated inside the PCC/precuneus, (pre)frontal, lateral parietal, as well as central temporal cortices and (ii) increments in FC between right parietal cortex and left insula (Ward et al., 2014). Moreover, in AD, resting state activity decreases were found to involve (i) DMN activity inside the PCC/precuneus, frontal, occipital, parietal, and (pre)frontal cortices and (ii) DMN activity between left hippocampus – prefrontal, dorsolateral cortex/PCC

– left frontoparietal cortices (Zhong et al., 2014). These outcomes point to the occurrence of possible compensatory forms rising in the beginning phases of the infection that are situated in a few DMN regions (Mevel et al., 2011).

On the other hand, aMCI and AD patients with high cognitive reserves demonstrated higher movement in task-related brain zones and expanded deactivations inside the DMN (PCC/precuneus, front cingulate) contrasted with those with low intellectual reserves (Solé-Padullés et al., 2009, Yamashita et al., 2019). This more prominent reallocation of handling assets from the DMN to cerebrum territories legitimately occupied with the test errand could reflect expanded redesign of useful compensatory assets in patients with high psychological reserves. To summarize, higher cognitive reserve capacities permit a more-with-less method of brain function in normal aging and makes up for neurotic procedures as they show up (Rombouts et al., 2005).

One other objective of the current studies evaluating the impacts of AD on the DMN is to disentangle biomarkers that might be valuable for the early diagnosis of the disease. The interruption of the hippocampus or PCC availability could be a decent applicant, as it increases as the illness progresses. Lower deactivations inside the entire DMN, and particularly inside (average) parietal territories, were also seen as related to change from aMCI. Furthermore, Koch et al. proposed that the utilization of multivariate investigations joining proportions of the movement of explicit DMN zones to proportions of the interconnectivity between these locales improved the determination precision. Strikingly, utilizing this methodology, the infection design seen in patients with AD could be distinguished in a great extent from that of aMCI patients, recommending that such a mix of resting state scans might be appropriate to diagnose AD at an early stage.

Past studies have given an enlarging backing to a preferential alteration of the parts of DMN in AD, however. In any case, the purpose behind the prevalent powerlessness of these

areas stays indistinct. As per Buckner et al., cortical center points might be mainly influenced in AD considering their persistent high standard movement and related metabolism, which may prompt expanded helplessness (quite to beta-amyloid testimony). This speculation is backed by studies demonstrating a connection between amyloid deposition and impaired DMN function in older individuals without dementia. Further multimodal examinations in all-risk subjects and AD patients are expected to be even more likely to comprehend this fascinating cover between the DMN and the dissemination of beta-amyloid testimony inside the brain (Sheline et al., 2010).

Considering that there are similar trends within the graphs and that there are some significant results for some of the outcomes of the P-values from the multiple linear regression analyses, it is possible to say that this study is a positive step to achieve desired results with the current hypothesis with further research. As pointed out earlier, the DMN contains the precuneus or PCC. The functional connectivity between the hippocampus (which is in the MT) and the PCC appeared to be impaired with AD. Following reduction in visual processing areas, AD patients starts exhibiting memory-induced alterations or decrease in resting state activation of MT (Golby et al., 2005). The hippocampal atrophy instituted episodic memory and functional perturbation impairment due to the disruption of the cingulum bundle (Agosta et al., 2012, Sorg et al., 2007, Wu et al., 2011, Yamasaki et al., 2019, Zhang et al., 2009).

6.2 Conclusion

The results from the current study, although like the results from previous studies, are statistically insignificant. In other words, none of the results were able to explain the graphs with the AGExGROUP feature, and only the DMN-mALFF results were able to explain the GROUP feature. 4 out of 6 measures (DMN-mALFF, DMN-ReHo, MV-mALFF, and MV-ReHo) were able to explain the graphs with the AGE feature.

This does not necessarily mean these features cannot be used as biomarkers. There are multiple reasons why the feature with age and group interaction from the formula was not significant for the 6 graphs. One of the main reasons is the quality of the fMRI scans. After realignment, six motion parameters were used to calculate frame displacement values for all scans. A standard deviation value of 2 was used as a threshold after taking the Z scores of the motion parameters. Even with 2 as the standard deviation, more than half of the dataset was excluded because of the high motion within the scans. Furthermore, some subjects had corrupted fMRI and anatomical scans that had to be removed. Even with the low quality of the fMRI scans, expected patterns within the graphs were seen.

Total number of 28 scans had to be removed due to following reasons: corrupted fMRI/T1 scans, inconsistent number of time points in fMRI scans, too many head motion effects after calculating frame displacement using the 6 motion parameters, and normalization issues. After the removal of scans, there were a total of 31 HCs and 30 AD patients left after pre-processing, which had either had single or multiple scans for each subject (total number of 79 scans for HC and 76 scans for AD patients). Because of the data's limitations, a presumption of accepting each scan as an individual subject was made, but not even this was enough to be able to generate significance with the equation in Figure 4.4.

Also, the scans were acquired at different sites. This could have caused variability in the data. Each MRI scanner has a unique noise coming from its components, called the scanner noise. Like the effects from head motion, this can cause certain values within the scan to elevate and cause false negative results.

Another reason could be the age range of the groups that might have cause insignificant results. Differences in the age ranges for each group might have affected the slopes of the graphs, which might have created insignificant results. For AD patients, this range is between 55 to 88, while for HC it is between 65 to 90. Slopes being affected might have changed the

pattern of the line generated by the multiple linear regression analysis, thus affecting the significance of the result.

The last reason for non-significant statistical results could be the absent information of the data. There was no information about the stage of the disease for each AD patient. This could have caused variability in the data. This can also be seen in the differences between scores for patients with the same age and condition, as shown in the generated graphs (Chapter 5). Overall, resting state functional magnetic resonance imaging as a neuroimaging method has great potential to increase diagnoses and prognoses of AD. Using the modality and various analyses techniques, it is possible to find neuroimaging biomarkers for not only AD, but also other cognitive disorders for early detection. Although there is great potential, future research needs to be done on the topic.

REFERENCES

Agosta F, Pievani M, Geroldi C, Copetti M, Frisoni GB, Filippi M. Resting state fMRI in Alzheimer's disease: Beyond the default mode network. Neurobiol Aging. 2012;33(8):1564-1578. doi:10.1016/j.neurobiolaging.2011.06.007

Armstrong RA. Visual field defects in Alzheimer's disease patients may reflect differential pathology in the primary visual cortex. Optom Vis Sci. 1996;73(11):677-682. doi:10.1097/00006324-199611000-00001

Armstrong RA. Alzheimer's disease and the eye. J Optom. 2009;2(3):103-111. doi:10.3921/joptom.2009.103

Azeez A. Developmental and Sex Modulated Neurological Alterations in Autism Spectrum Disorder. New Jersey Inst Technol. Published online 2019:129.

Azeez AK, Biswal BB. A Review of Resting-State Analysis Methods. Neuroimaging Clin N Am. 2017;27(4):581-592. doi:10.1016/j.nic.2017.06.001

Badhwar AP, Tam A, Dansereau C, Orban P, Hoffstaedter F, Bellec P. Resting-state network dysfunction in Alzheimer's disease: A systematic review and meta-analysis. Alzheimer's Dement Diagnosis, Assess Dis Monit. 2017;8:73-85. doi:10.1016/j.dadm.2017.03.007

Bamberg E, Noda K, Läuger P. Single-channel parameters of gramicidin a,b, and c. BBA – Biomembr. 1976;419(2):223-228. doi:10.1016/0005-2736(76)90348-5

Basil G, Madhavan K, Komotar RJ, Carrillo R, Levi AD. The Utility of Magnetic Resonance Imaging-compatible Pacemakers in Neurosurgical Patients. Cureus. 2018;10(9). doi:10.7759/cureus.3374

Bayram E, Caldwell JZK, Banks SJ. Current understanding of magnetic resonance imaging biomarkers and memory in Alzheimer's disease. Alzheimer's Dement Transl Res Clin Interv. 2018;4:395-413. doi:10.1016/j.trci.2018.04.007

Beach TG, McGeer EG. Cholinergic fiber loss occurs in the absence of synaptophysin depletion in Alzheimer's disease primary visual cortex. Neurosci Lett. 1992;142(2):253-256. doi:10.1016/0304-3940(92)90385-K

Beckmann CF, DeLuca M, Devlin JT, Smith SM. Investigations into resting-state connectivity using independent component analysis. Philos Trans R Soc B Biol Sci. 2005;360(1457):1001-1013. doi:10.1098/rstb.2005.1634

Berron D, van Westen D, Ossenkoppele R, Strandberg O, Hansson O. Medial temporal lobe connectivity and its associations with cognition in early Alzheimer's disease. Brain. 2020;143(4):1233-1248. doi:10.1093/brain/awaa068

Bi XA, Jiang Q, Sun Q, Shu Q, Liu Y. Analysis of Alzheimer's Disease Based on the Random Neural Network Cluster in fMRI. Front Neuroinform. Published online 2018. doi:10.3389/fninf.2018.00060

Biswal, B., Yetkin, F. Z., Haughton, V. M., & Hyde, J. S. (1995). Functional connectivity in the motor cortex of resting human brain using echo-planar MRI. Magnetic resonance in medicine, 34(4), 537–541. https://doi.org/10.1002/mrm.1910340409

Biswal BB, Van Kylen J, Hyde JS. Simultaneous assessment of flow and BOLD signals in resting-state functional connectivity maps. NMR Biomed. 1997;10(4-5):165-170. doi:10.1002/(sici)1099-1492(199706/08)10:4/5<165::aid-nbm454>3.0.co;2-7

Bokde ALW, Lopez-Bayo P, Meindl T, et al. Functional connectivity of the fusiform gyrus during a face-matching task in subjects with mild cognitive impairment. Brain. 2006;129(5):1113-1124. doi:10.1093/brain/awl051

Boynton GM, Engel SA, Glover GH, Heeger DJ. Linear systems analysis of functional magnetic resonance imaging in human V1. J Neurosci. 1996;16(13):4207-4221. doi:10.1523/jneurosci.16-13-04207.1996

Buckner RL, Andrews-Hanna JR, Schacter DL. The brain's default network: Anatomy, function, and relevance to disease. Ann N Y Acad Sci. 2008;1124:1-38. doi:10.1196/annals.1440.011

Buckner RL, Krienen FM, Yeo BTT. Opportunities and limitations of intrinsic functional connectivity MRI. Nat Neurosci. 2013;16(7):832-837. doi:10.1038/nn.3423

Calhoun VD, Adali T, Hansen LK. ICA of functional MRI data: an overview. Proc …. Published online 2003. doi:10.1.1.3.7473

Cerquera-Jaramillo MA, Nava-Mesa MO, González-Reyes RE, Tellez-Conti C, De-La-Torre A. Visual features in Alzheimer's disease: From basic mechanisms to clinical overview. Neural Plast. 2018;2018. doi:10.1155/2018/2941783

Chen K, Azeez A, Chen DY, Biswal BB. Resting-State Functional Connectivity: Signal Origins and Analytic Methods. Neuroimaging Clin N Am. Published online 2020. doi:10.1016/j.nic.2019.09.012

Chen S, Ross TJ, Zhan W, et al. Group independent component analysis reveals consistent resting-state networks across multiple sessions. Brain Res. 2008;1239:141-151. doi:10.1016/j.brainres.2008.08.028

Cohen MS. Parametric analysis of fMRI data using linear systems methods. Neuroimage. 1997;6(2):93-103. doi:10.1006/nimg.1997.0278

Cox RW. AFNI: Software for analysis and visualization of functional magnetic resonance neuroimages. Comput Biomed Res. 1996;29(3):162-173. doi:10.1006/cbmr.1996.0014

Damoiseaux JS. Resting-state fMRI as a biomarker for Alzheimer's disease. Alzheimer's Res Ther. Published online 2012. doi:10.1186/alzrt106

Desgranges B, Mevel K, Chételat G, Eustache F. The default mode network in healthy aging and Alzheimer's disease. Int J Alzheimers Dis. 2011;2011. doi:10.4061/2011/535816

Di X, Wölfer M, Amend M, et al. Interregional causal influences of brain metabolic activity reveal the spread of aging effects during normal aging. Hum Brain Mapp. 2019;40(16):4657-4668. doi:10.1002/hbm.24728

Fischer, F. U., Wolf, D., Fellgiebel, A., & Alzheimer's Disease Neuroimaging Initiative* (2019). Connectivity and morphology of hubs of the cerebral structural connectome are associated with brain resilience in AD- and age-related pathology. Brain imaging and behavior, 13(6), 1650–1664. https://doi.org/10.1007/s11682-019-00090-y

Fox J, Bouchet-Valat M (2020). Rcmdr: R Commander. R package version 2.62, http://socserv.socsci.mcmaster.ca/jfox/Misc/Rcmdr/.

Fox MD, Raichle ME. Spontaneous fluctuations in brain activity observed with functional magnetic resonance imaging. Nat Rev Neurosci. 2007;8(9):700-711. doi:10.1038/nrn2201

Friston KJ, Frith C, Frackowiak RSJ, Turner R. Characterizing dynamic brain responses with fMRI. Neuroimage. 1995;2:166-172.

Friston KJ, Holmes AP, Worsley KJ, Poline J -P, Frith CD, Frackowiak RSJ. Statistical parametric maps in functional imaging: A general linear approach. Hum Brain Mapp. 1994;2(4):189-210. doi:10.1002/hbm.460020402

Friston KJ. Functional and effective connectivity in neuroimaging: A synthesis. Hum Brain Mapp. 1994;2(1-2):56-78. doi:10.1002/hbm.460020107

Friston KJ, Williams S, Howard R, Frackowiak RSJ, Turner R. Movement-related effects in fMRI time-series. Magn Reson Med. 1996;35(3):346-355. doi:10.1002/mrm.1910350312

Gardini S, Venneri A, Sambataro F, et al. Increased Functional Connectivity in the Default Mode Network in Mild Cognitive Impairment: A Maladaptive Compensatory Mechanism Associated with Poor Semantic Memory Performance. J Alzheimer's Dis. 2015;45(2):457-470. doi:10.3233/JAD-142547

Giffard B, Laisney M, Mézenge F, de la Sayette V, Eustache F, Desgranges B. The neural substrates of semantic memory deficits in early Alzheimer's disease: Clues from semantic priming effects and FDG-PET. Neuropsychologia. Published online 2008. doi:10.1016/j.neuropsychologia.2007.12.031

Gilboa A, Ramirez J, Köhler S, Westmacott R, Black SE, Moscovitch M. Retrieval of autobiographical memory in Alzheimer's disease: Relation to volumes of medial temporal lobe and other structures. Hippocampus. 2005;15(4):535-550. doi:10.1002/hipo.20090

Glover GH. Overview of functional magnetic resonance imaging. Neurosurg Clin N Am. 2011;22(2):133-139. doi:10.1016/j.nec.2010.11.001

Golby A, Silverberg G, Race E, et al. Memory encoding in Alzheimer's disease: An fMRI study of explicit and implicit memory. Brain. Published online 2005. doi:10.1093/brain/awh400

Grajski KA, Bressler SL. Differential medial temporal lobe and default-mode network functional connectivity and morphometric changes in Alzheimer's disease. NeuroImage Clin. 2019;23(February 2018):101860. doi:10.1016/j.nicl.2019.101860

Greicius MD, Srivastava G, Reiss AL, Menon V. Default-mode network activity distinguishes Alzheimer's disease from healthy aging: Evidence from functional MRI. Proc Natl Acad Sci U S A. 2004;101(13):4637-4642. doi:10.1073/pnas.0308627101

Hafiz R. Subject and group level changes and comparison in functional connectivity under low vs . high cognitively demanding naturalistic viewing conditions using fmri New Jersey Inst Technol. Published online 2017. https://digitalcommons.njit.edu/theses/34

He Y, Wang L, Zang Y, et al. Regional coherence changes in the early stages of Alzheimer's disease: A combined structural and resting-state functional MRI study. Neuroimage. 2007;35(2):488-500. doi:10.1016/j.neuroimage.2006.11.042

Heeger DJ, Ress D. What does fMRI tell us about neuronal activity? Nat Rev Neurosci. 2002;3(2):142-151. doi:10.1038/nrn730

Higham, D. J., & Higham, N. J. (2016). MATLAB guide (Vol. 150). Siam.

Hippius, H., & Neundörfer, G. (2003). The discovery of Alzheimer's disease. Dialogues in clinical neuroscience, 5(1), 101–108.

Huettel SA, Song AW, McCarthy G. Functional Magnetic Resonance Imaging, Third Edition.; 2014. doi:10.1088/1475-7516/2003/08/005

Huf W, Kalcher K, Boubela RN, et al. On the generalizability of resting-state fMRI machine learning classifiers. Front Hum Neurosci. 2014;8(JULY):1-11. doi:10.3389/fnhum.2014.00502

Ikonomovic MD, Mufson EJ, Wuu J, Bennett DA, DeKosky ST. Reduction of choline acetyltransferase activity in primary visual cortex in mild to moderate Alzheimer's disease. Arch Neurol. 2005;62(3):425-430. doi:10.1001/archneur.62.3.425

Jiang L, Zuo XN. Regional Homogeneity: A Multimodal, Multiscale Neuroimaging Marker of the Human Connectome. Neuroscientist. 2016;22(5):486-505. doi:10.1177/1073858415595004

Jenkinson, M., Beckmann, C. F., Behrens, T. E. J., Woolrich, M. W., & Smith, S. M. (2012). FSL. NeuroImage, 62(2), 782–790. https://doi.org/10.1016/j.neuroimage.2011.09.015

Johnson, K. A., Fox, N. C., Sperling, R. A., & Klunk, W. E. (2012). Brain imaging in Alzheimer disease. Cold Spring Harbor perspectives in medicine, 2(4), a006213. https://doi.org/10.1101/cshperspect.a006213

Khazaee A, Ebrahimzadeh A, Babajani-Feremi A. Identifying patients with Alzheimer's disease using resting-state fMRI and graph theory. Clin Neurophysiol. Published online 2015. doi:10.1016/j.clinph.2015.02.060

Koch W, Teipel S, Mueller S, et al. Diagnostic power of default mode network resting state fMRI in the detection of Alzheimer's disease. Neurobiol Aging. 2012;33(3):466-478. doi:10.1016/j.neurobiolaging.2010.04.013

Kusne Y, Wolf AB, Townley K, Conway M, Peyman GA. Visual system manifestations of Alzheimer's disease. Acta Ophthalmol. 2017;95(8):e668-e676. doi:10.1111/aos.13319

Lajoie I, Nugent S, Debacker C, et al. Application of calibrated fMRI in Alzheimer's disease. NeuroImage Clin. 2017;15(April):348-358. doi:10.1016/j.nicl.2017.05.009

Lee MH, Smyser CD, Shimony JS. Resting-state fMRI: A review of methods and clinical applications. Am J Neuroradiol. Published online 2013. doi:10.3174/ajnr.A3263

Leuba G, Kraftsik R. Visual cortex in Alzheimer's disease: Occurencee of neuronal death and glial proliferation, and correlation with pathological hallmarks. Neurobiol Aging. 1994;15(1):29-43. doi:10.1016/0197-4580(94)90142-2

Li SJ, Li Z, Wu G, Zhang MJ, Franczak M, Antuono PG. Alzheimer disease: Evaluation of a functional MR imaging index as a marker. Radiology. 2002;225(1):253-259. doi:10.1148/radiol.2251011301

Liu Y, Wang K, YU C, et al. Regional homogeneity, functional connectivity and imaging markers of Alzheimer's disease: A review of resting-state fMRI studies. Neuropsychologia.2008;46(6):1648-1656. doi:10.1016/j.neuropsychologia.2008.01.027

Marchitelli R, Aiello M, Cachia A, et al. Simultaneous resting-state FDG-PET/fMRI in Alzheimer Disease: Relationship between glucose metabolism and intrinsic activity. Neuroimage. 2018;176(April):246-258. doi:10.1016/j.neuroimage.2018.04.048

Márquez F, Yassa MA. Neuroimaging Biomarkers for Alzheimer's Disease. Mol Neurodegener. 2019;14(1):1-14. doi:10.1186/s13024-019-0325-5

Mendez, M. F., Mendez, M. A., Martin, R., Smyth, K. A., & Whitehouse, P. J. (1990). Complex visual disturbances in Alzheimer's disease. Neurology, 40(3 Pt 1), 439–443. https://doi.org/10.1212/wnl.40.3_part_1.439

Onyike C. U. (2016). Psychiatric Aspects of Dementia. Continuum (Minneapolis, Minn.), 22(2 Dementia), 600–614. https://doi.org/10.1212/CON.0000000000000302

Poldrack RA, Nichols T, Mumford J. Handbook of Functional MRI Data Analysis.; 2011. doi:10.1017/cbo9780511895029

Qi H, Liu H, Hu H, He H, Zhao X. Primary Disruption of the Memory-Related Subsystems of the Default Mode Network in Alzheimer's Disease: Resting-State Functional Connectivity MRI Study. Front Aging Neurosci. 2018;10(October):1-10. doi:10.3389/fnagi.2018.00344

Dale Purves, George J. Augustine, David Fitzpatrick, William C. Hall, Anthony-Samuel LaMantia Richard D. Mooney, Michael L. Platt, Leonard E. White Neuroscience 6th edition. Sunderland, Mass: Sinauer Associates Publishers..;2018

Ridha BH, Barnes J, Van De Pol LA, et al. Application of automated medial temporal lobe atrophy scale to Alzheimer disease. Arch Neurol. 2007;64(6):849-854. doi:10.1001/archneur.64.6.849

Rombouts SARB, Barkhof F, Goekoop R, Stam CJ, Scheltens P. Altered resting state networks in mild cognitive impairment and mild Alzheimer's disease: An fMRI study. Hum Brain Mapp. 2005;26(4):231-239. doi:10.1002/hbm.20160

Rossor MN, Fox NC, Mummery CJ, Schott JM, Warren JD. The diagnosis of young-onset dementia. Lancet Neurol. 2010;9(8):793-806. doi:10.1016/S1474-4422(10)70159-9

Sheline YI, Raichle ME, Snyder AZ, et al. Amyloid Plaques Disrupt Resting State Default Mode Network Connectivity in Cognitively Normal Elderly. Biol Psychiatry. 2010;67(6):584-587. doi:10.1016/j.biopsych.2009.08.024

Smitha KA, Akhil Raja K, Arun KM, et al. Resting state fMRI: A review on methods in resting state connectivity analysis and resting state networks. Neuroradiol J. 2017;30(4):305-317. doi:10.1177/1971400917697342

Solé-Padullés C, Bartrés-Faz D, Junqué C, et al. Brain structure and function related to cognitive reserve variables in normal aging, mild cognitive impairment and Alzheimer's disease. Neurobiol Aging. Published online 2009. doi:10.1016/j.neurobiolaging.2007.10.008

Sorg C, Riedl V, Mühlau M, et al. Selective changes of resting-state networks in individuals at risk for Alzheimer's disease. Proc Natl Acad Sci U S A. 2007;104(47):18760-18765. doi:10.1073/pnas.0708803104

Tepmongkol S, Hemrungrojn S, Dupont P, et al. Early prediction of donepezil cognitive response in Alzheimer's disease by brain perfusion single photon emission tomography. Brain Imaging Behav. Published online 2019. doi:10.1007/s11682-019-00182-9

van der Miesen M, Lindquist M, Wager T. Neuroimaging-based biomarkers for pain: state of the field and current directions. PAIN Reports. 2019;4(4):e751. doi:10.1097/PR9.0000000000000751

Van Dijk KRA, Hedden T, Venkataraman A, Evans KC, Lazar SW, Buckner RL. Intrinsic functional connectivity as a tool for human connectomics: Theory, properties, and optimization. J Neurophysiol. 2010;103(1):297-321. doi:10.1152/jn.00783.2009

Wang L, Zang Y, He Y, et al. Changes in hippocampal connectivity in the early stages of Alzheimer's disease: Evidence from resting state fMRI. Neuroimage. Published online 2006. doi:10.1016/j.neuroimage.2005.12.033

Ward AM, Schultz AP, Huijbers W, Van Dijk KRA, Hedden T, Sperling RA. The parahippocampal gyrus links the default-mode cortical network with the medial temporal lobe memory system. Hum Brain Mapp. 2014;35(3):1061-1073. doi:10.1002/hbm.22234

Woo C-W, Chang LJ, Lindquist MA, Wager TD. Building better biomarkers: brain models in translational neuroimaging. Nat Neurosci. 2017;20(3):365-377. doi:10.1038/nn.4478

Woo C-W, Wager TD. Neuroimaging-based biomarker discovery and validation. Pain. 2015;156(8):1379-1381. doi:10.1097/j.pain.0000000000000223

Wu X, Li R, Fleisher AS, et al. Altered default mode network connectivity in Alzheimer's disease-A resting functional MRI and Bayesian network study. Hum Brain Mapp. 2011;32(11):1868-1881. doi:10.1002/hbm.21153

Yamasaki T, Aso T, Kaseda Y, et al. Decreased stimulus-driven connectivity of the primary visual cortex during visual motion stimulation in amnestic mild cognitive impairment: An fMRI study. Neurosci Lett. 2019;711. doi:10.1016/j.neulet.2019.134402

Yamashita K ichiro, Uehara T, Prawiroharjo P, et al. Functional connectivity change between posterior cingulate cortex and ventral attention network relates to the impairment of orientation for time in Alzheimer's disease patients. Brain Imaging Behav. 2019;13(1):154-161. doi:10.1007/s11682-018-9860-x

Yang L, Yan Y, Li Y, et al. Frequency-dependent changes in fractional amplitude of low-frequency oscillations in Alzheimer's disease: a resting-state fMRI study. Brain Imaging Behav. Published online 2019. doi:10.1007/s11682-019-00169-6

Yetkin FZ, Rosenberg RN, Weiner MF, Purdy PD, Cullum CM. FMRI of working memory in patients with mild cognitive impairment and probable Alzheimer's disease. Eur Radiol. Published online 2006. doi:10.1007/s00330-005-2794-x

Yu E, Liao Z, Mao D, et al. Directed Functional Connectivity of Posterior Cingulate Cortex and Whole Brain in Alzheimer's Disease and Mild Cognitive Impairment. Curr Alzheimer Res. 2016;14(6):628-635. doi:10.2174/1567205013666161201201000

Zang Y, Jiang T, Lu Y, He Y, Tian L. Regional homogeneity approach to fMRI data analysis. Neuroimage. 2004;22(1):394-400. doi:10.1016/j.neuroimage.2003.12.030

Zhang, H. Y., Wang, S. J., Xing, J., Liu, B., Ma, Z. L., Yang, M., Zhang, Z. J., & Teng, G. J. (2009). Detection of PCC functional connectivity characteristics in resting-state fMRI in mild Alzheimer's disease. Behavioural brain research, 197(1), 103–108. https://doi.org/10.1016/j.bbr.2008.08.012

Zhang Z, Liu Y, Jiang T, et al. Altered spontaneous activity in Alzheimer's disease and mild cognitive impairment revealed by Regional Homogeneity. Neuroimage. 2012;59(2):1429-1440. doi:10.1016/j.neuroimage.2011.08.049

Zhong Y, Huang L, Cai S, et al. Altered effective connectivity patterns of the default mode network in Alzheimer's disease: An fMRI study. Neurosci Lett. Published online 2014. doi:10.1016/j.neulet.2014.06.043

Zou QH, Zhu CZ, Yang Y, et al. An improved approach to detection of amplitude of low-frequency fluctuation (ALFF) for resting-state fMRI: Fractional ALFF. J Neurosci Methods. 2008;172(1):137-141. doi:10.1016/j.jneumeth.2008.04.012